

T-1887

RHEOLOGY OF FOAM CEMENT

by

Ali Mohsen Al-Mashat

ARTHUR LAKES LIBRARY
COLORADO SCHOOL of MINES
GOLDEN, COLORADO 80401

ProQuest Number: 10796121

All rights reserved

INFORMATION TO ALL USERS

The quality of this reproduction is dependent upon the quality of the copy submitted.

In the unlikely event that the author did not send a complete manuscript and there are missing pages, these will be noted. Also, if material had to be removed, a note will indicate the deletion.



ProQuest 10796121

Published by ProQuest LLC (2019). Copyright of the Dissertation is held by the Author.

All rights reserved.

This work is protected against unauthorized copying under Title 17, United States Code
Microform Edition © ProQuest LLC.

ProQuest LLC.
789 East Eisenhower Parkway
P.O. Box 1346
Ann Arbor, MI 48106 – 1346

A Dissertation submitted to the Faculty and the Board of Trustees of the Colorado School of Mines in partial fulfillment of the requirements for the degree of Doctor of Philosophy (Petroleum Engineering).

Signed: *Ali Al-Mashat*
Ali Mohsen Al-Mashat

Golden, Colorado

Date: Nov - 23 -, 1976

Approved: *Bill Mitchell*
B.J. Mitchell
Thesis Advisor

D.M. Bass
D.M. Bass
Head of Department of
Petroleum Engineering

Golden, Colorado

Date: Nov 23,, 1976

ABSTRACT

Analysis of experimental data together with theoretical discussion pertinent to foam cement permit definite conclusions regarding certain rheological properties of foam cement. Foam cement in these experiments was dynamically generated by blending air, cement slurry, and a surface active agent within a device called a foam cement generator, which is in contrast with the familiar batch method which utilizes a cup and blender. The range of foam cement qualities was from zero to 70 percent. Flow of foam cement was investigated in two capillary size tubes which had diameters of 0.093 and 0.132 inches.

The emulsion theories of Einstein and Hatschek are applied to foam cement in an attempt to build a physical model for the explanation of the flow behavior of foam cement. The Bingham plastic and the power law models were chosen to represent the flow properties of viscosity and yield of foam cement. Pressure differentials across the capillary size tubes were measured at several foam cement qualities and flow rates. Logarithmic plots of shear stress versus shear rate

are presented for six foam cement quality ranges. Empirical formulas relating yield point, plastic viscosity, consistency index, and flow behavior index for foam cement qualities are presented.

TABLE OF CONTENTS

	<u>Page</u>
Abstract -----	ii
Table of Contents -----	v
List of Tables -----	vii
List of Figures -----	viii
Acknowledgement -----	x
Introduction -----	1
Chapter 1. Review of Previous Work -----	5
Summary of Previous Work and its Relationship to This Work -----	21
Chapter 2. Theory -----	24
Bingham Plastic Fluid -----	25
Pseudo Plastic and Dilatant Fluid -----	26
Chapter 3. Experiments and Apparatus -----	41
Cement Injection System -----	41
Foaming Agent Injection System -----	42
Air Injection System -----	42
Air Measuring System -----	43
Foam Cement Generation System -----	43
Flow Tube System -----	43
Pressure Measuring System -----	44
Differential Pressure Measuring System -----	44
Temperature Monitoring System -----	45

<u>Table of Contents continued</u>	<u>Page</u>
Calibration -----	45
Technique -----	47
Chapter 4. Results and Discussion -----	50
Conclusions -----	51
Nomenclature -----	54
Bibliography -----	55

LIST OF TABLES

	<u>Page</u>
Table 1. Dimension of Flow Tube -----	59
2. Flow Tube Calibration -----	59
3. Flow Tube Calibration data -----	60
4. Foam Cement Flow Data $0.3 < \Gamma < 0.4$ -----	63
5. Foam Cement Flow Data $0.4 < \Gamma < 0.45$ -----	66
6. Foam Cement Flow Data $0.45 < \Gamma < 0.5$ -----	69
7. Foam Cement Flow Data $0.5 < \Gamma < 0.55$ -----	72
8. Foam Cement Flow Data $0.55 < \Gamma < 0.6$ -----	75
9. Foam Cement Flow Data $0.6 < \Gamma < 0.65$ -----	77

LIST OF FIGURES

	<u>Page</u>
Figure 1. Continuous Distribution Curve -----	78
2. Apparent Viscosity and Different Rate of Shear of Emulsions -----	78
3. Schematic Representation of the Principal Types of Surface Tension Concentration Curves -----	79
4. The Range of Surface Tensions Found in Solutions of Most Surface Active Compounds -----	79
5. Solid Particles Suspended in Gas-Liquid Boundary by Surface Tension-----	80
6. Relation Between the Three Angles β , ψ , and θ_R -----	80
7. Rabinowitsch Flow Model -----	81
8. High Pressure Temperature Viscometer -----	82
9. Plot of Pump Flow Rate versus Dial Number -----	83
10. Calibration of Tubes -----	84
11. Viscosity Calibration Curve -----	85
12. Foam Cement Rheology Diagram $0.3 < \Gamma < 0.4$ -----	86
13. Foam Cement Rheology Diagram $0.4 < \Gamma < 0.45$ ---	87
14. Foam Cement Rheology Diagram $0.45 < \Gamma < 0.5$ ---	88

<u>List of Figures</u> continued	<u>Page</u>
Figure 15. Foam Cement Rheology Diagram $0.5 < \Gamma < 0.55$ ---	89
16. Foam Cement Rheology Diagram $0.55 < \Gamma < 0.6$ ---	90
17. Foam Cement Rheology Diagram $0.6 < \Gamma < 0.65$ ---	91
18. Foam Cement Viscosity (Tube I.D.-0.132)-----	92
19. Foam Cement Viscosity (Tube I.D.-0.093)-----	93
20. Foam Cement Viscosity $0.3 < \Gamma < 0.4$ -----	94
21. Foam Cement Viscosity $0.4 < \Gamma < 0.45$ -----	95
22. Foam Cement Viscosity $0.45 < \Gamma < 0.5$ -----	96
23. Foam Cement Viscosity $0.5 < \Gamma < 0.55$ -----	97
24. Foam Cement Viscosity $0.55 < \Gamma < 0.6$ -----	98
25. Foam Cement Viscosity $0.6 < \Gamma < 0.65$ -----	99
26. Yield Stress of Foam Cement -----	100
27. Plastic Viscosity of Foam Cement -----	101
28. Flow Behavior Index of Foam Cement -----	102
29. Consistency Index of Foam Cement-----	103
30. Surface Tension of Howco and Tap Water -----	104

ACKNOWLEDGMENT

The author wishes to express his appreciation to the many people at the Colorado School of Mines who helped with this dissertation. Dr. B.J. Mitchell acted as research advisor throughout this investigation. His guidance and constructive criticism were invaluable. Dr. D.M. Bass and Dr. C.A. Kohlhaas graciously read and criticized the manuscript for content and clarity. In addition, appreciation is also due to the Amoco Production Company, Chevron - West, Chevron Oil Field Research Company, El Paso Natural Gas Company, Exxon, and Getty, for their financial support.

Many thanks are due to Dr. Bass, Dr. Kohlhaas, Dr. Mitchell, Dr. Whitman, and Prof. Dickinson, for their tolerant approach to the direction of this research and for their inspirational assistance and valuable suggestions; to Jim Boze for his help in erecting the experimental equipment in addition to obtaining and repairing parts thereof.

Finally I wish to thank those of the Ministry of Higher Education and Scientific Research of Iraq for their generous assistance throughout my graduate studies in the United States.

INTRODUCTION

We are all familiar with foam as it occurs in every day life and hardly a day goes by without our encountering it in one form or another. Some foams such as those encountered in water pollution and on trays in oil refineries are a nuisance, but others such as those that occur in beverages or fire fighting foam are desirable. Mineral engineers have used aqueous foam as a means of separating minerals.

In the petroleum industry, foams were first encountered in gas/oil separation. There foam was found spread over the incoming oil and inhibited the separation of the gas from the oil. The drilling of oil wells has been carried out successfully with the use of the foam as a drilling fluid. In this case, its light weight, its low penetration into permeable rock and its ability to carry cuttings to the surface proved its value as a drilling fluid. The properties of foams low fluid losses, high sand carrying, sand suspension capability, high effective viscosities, and low friction losses make it a desirable fluid for use as a

fracturing fluid. Foam has been suggested as a displacing agent in conjunction with waterflooding of oil reservoirs. The behavior of foam flowing through pipe has been studied by several investigators and it has been shown that within certain quality ranges the foam behaves as a Newtonian fluid and above that quality range, foam behaves as a Bingham-plastic fluid. Einstein (1906) and Hatschek (1910) point out foam should be treated as a single-phase fluid with viscosities significantly greater than either phase. Mitchell (1969) used these theories and experimental data to depict analytical flow characteristics of foam.

Solid foam, at present has greater commercial importance, every one is familiar with foam rubber, polyurethane foam, etc. In all true foams whether the films are liquid or solid, each bubble is closed; that is, it has no gas filled channels connecting it with the neighboring bubbles (also known as a cell in solid foam). When such connections exist, the foam is considered as a sponge. The sponge state requires both phases (that is, gas and liquid) to be continuous, whereas, in the foam state the gas occurs as a discontinuous phase and the liquid occurs as a continuous phase.

Foam cement according to the preceding paragraph can be defined as an agglomeration of gas bubbles separated by a thin layer of cement slurry. The cement slurry and

the surface active agents form the continuous phase, while the gas which appears as bubbles is the discontinuous phase. Foam cement quality which is the ratio of gas volume to the total volume (gas volume and liquid volume) in this study is found between zero and 70 percent. In the laboratory, foam cement is successfully generated by controlled injection of a gas into a line carrying cement slurry. Surfactant content is commonly 0.5 to 0.7 percent of the cement slurry volume. Stability is increased by the addition of surfactant up to a concentration of 1 percent. Such a foam forms homogeneous mixtures with a narrow range of bubble size.

Foam cement can be used in the field for the following purposes:

1. To separate formations behind the casing which prevents interformational flow of liquids and permits production from a specific zone.
2. To afford additional support for the casing either by physical bracing or the reduction of formation stress that may be imposed on the pipe.
3. To retard corrosion by minimizing the contact of the pipe and possible corrosive formation water.

Fluid properties of the foam cement for field processes must be available for the calculations involved in the planning of these processes. Since foam cement is a Non-Newtonian fluid, two parameters are commonly used to define

flow characteristics. Two such parameters are denoted by the symbols n' and k' , which are the flow behavior index and consistency index, respectively, for use in the Power Law model, and plastic viscosity (μ_p) and yield point (τ_y) are used with the Bingham Plastic model.

Either of these two models and their parameters permit the calculation of the Reynold's number and the Fanning friction factor which in turn assists in the planning and execution of field processes pertinent to foam cement. Thus, this study was designed and executed to experimentally depict these four parameters in regard to foam cement. Other noteworthy characteristics of foam cement are presented as a matter of general interest.

CHAPTER I. REVIEW OF PREVIOUS WORK

Sibree (1934) was one of the first investigators of the viscosity of foam. He conducted his experiment at room temperature and atmospheric pressure. A concentric cylinder, rotary viscometer was used to measure the shear forces and shear rate. He stated that the apparent viscosity of foam was higher than that of its constituents, and that it decreases with increasing shear rates.

Penney (1943) showed that above the yield stress, the apparent viscosity of foam can be measured between two plates and can be defined in the same manner as the viscosity of the liquid. He stated that foam can be represented by the Bingham plastic equation, which is

$$\tau - \tau_y = \mu_p \left(\frac{-dv}{dr} \right)$$

where τ = shear stress

τ_y = yield stress

μ_p = plastic viscosity

$\left(\frac{-dv}{dr} \right)$ = velocity gradient.

Using a friction factor versus Reynold's number plot, Grove et al (1951) measured the apparent viscosities of fire fighting foam having various expansion ratios (the ratio of foam density to liquid density) as a function of pressure and shear rate. They used a viscometer which measured drag through the extension of a spring in order to find the Fanning friction factor. Results indicated that at high shear rate, the apparent viscosity was independent of the shear rate. However, the apparent viscosities varied almost fifteen fold over the foam density range that was used (15-46 lbs/ft³, a quality range of 0.76 to 0.26).

Wise (1951) studied the flow resistance of fire-fighting foam through an iron pipe. He showed that foam behaved as does a pure pseudoplastic fluid. His equation relates apparent viscosity and density of foam, with rate of shear

$$\log (\mu_a \rho^2) = a \log \phi + b$$

in which μ_a = apparent viscosity

$$\rho = \text{density} = \rho_L(1-\Gamma) + \rho_g\Gamma$$

ϕ = rate of shear

a,b = empirical constants

Since density is related to foam quality, he modified the above equation to obtain:

$$\log \mu_a = \log \Gamma^2 + a' \log v + b'$$

where Γ = quality fraction

a',b' = constants

v = average linear velocity

Fried (1961) measured the viscosity of the foam by using both a modified rotational viscometer and a capillary tube. His results show that the viscosity of foam increases with increasing foam quality and the inside diameter of the tube.

Marsden and Khan (1965) measured foam viscosity at atmospheric pressure and room temperature by using a modified Fann rotational viscometer. They worked with foam qualities ranging from 70 to 96 percent. In their conclusions, they state that apparent viscosity of foam decreased with increasing shear rate and viscosity increases as foam quality increases. Further, they concluded that kinematic viscosity is independent of foam quality at a given shear rate while apparent viscosity increases with foam quality from 3 to 8 cps.

Marsden and Raza (1967) measured the viscosity of foam flowing through capillary tubes. They described foam as a pseudo-plastic fluid, and submitted data which show that below a certain critical flow rate which depends on foam quality and shear rate, the flow is Newtonian; and that above this critical flow rate, foam flows through a tube as a viscous plug, with most of the shear occurring at the tube wall. This result is contrary to others and is viewed with doubt.

These authors also reported that foam is a compressible fluid and Boyle's law can be applied; but they did not report

errors in the equation caused by gas solution, gas deviation, etc. Marsden and Raza also measured the streaming potentials, which is the voltage difference developed between the ends of a capillary tube through which a foam is forced to flow by an applied pressure differential. Their results show that for a given tube radius and a given foam quality, an approximate linear relationship exists between pressure differential and streaming potential. The slope of this line increases significantly with both tube inside diameter and foam quality. They also show that the flow rate does not affect the streaming potential curve at all. Streaming potential as high as 30 volts were reported.

The rheology of foam can be simulated by considering the rheology of similar suspensions of solid in liquid. Einstein (1906) was one of the first to view the rheology of a dispersed system analytically. His totally theoretical relationship which is most applicable to lower concentrations of solid particles is

$$\mu_f = \mu_l (1 + 2.5\Gamma)$$

where

μ_f = suspension viscosity

μ_l = liquid viscosity

Γ = suspension quality fraction

Gas bubbles in foam may be thought of as solid particles.

Sibree made another approach to the problem of the rheology of foam. He stated that the relationship between the apparent viscosity of foam, the viscosity of the continuous phase, and the volume fraction of the non-continuous phase in the liquid is of the form

$$\mu = \mu_1 \left\{ \frac{1}{1 - h\Gamma^{1/3}} \right\}$$

where h is a quality coefficient. This equation which suggests that foam demonstrates a strong non-Newtonian behavior was first suggested by Hatschek.

Raza related the pressure P , flow rate q , and foam quality Γ by the following equation

$$P = aq + b\Gamma - c$$

where a , b , and c are constants depending on the radius of the capillary tubes.

Mitchell (1969) showed with 905 laboratory data points taken with three flow tubes that foam may be represented by a Bingham plastic fluid model in the quality range of 54 to 95 percent and is Newtonian in behavior in the quality range from zero to 54 percent, and at a quality above 96 percent an air, water, surfactant foam will convert to a mist. He also showed that the viscosity of foam increases with increasing quality and decreases with increasing shear rate.

Mitchell also empirically derived two viscosity equations for the above-described two quality regions

$$\mu_f = \mu_1 \{1.0 + 3.6 \Gamma\} \quad 0 < \Gamma < 0.54$$

and

$$\mu_f = \mu_1 \left\{ \frac{1}{1.0 + \Gamma^{0.49}} \right\} \quad 0.54 < \Gamma < 0.96$$

where

μ_f = foam viscosity in cps

μ_1 = base liquid viscosity in cps

Γ = foam quality expressed as a fraction.

Krug (1971) presented a mathematical model and its solution for the application of foam in a drilling system consisting of a vertical-concentric pipe-hole arrangement with flow down the pipe and up the annulus. The mathematical model describing the flow of foam contained the Bingham plastic model developed by Mitchell (1969) and considered foam to be a compressible fluid. Two major equations were written describing the flow of the foam: foam flowing vertically downward within pipe and foam with rock chips flowing up within an annulus.

Krug and Mitchell's (1972) modifications in existing single-phase fluid-flow equations account for both the compressibility of gas within the foam and the resulting changes in the viscosity. The resultant equations were applicable to the circulation of foam within a wellbore; however, these

equations were limited to laminar flow and lacked full scale testing.

Abbott (1974) in his work ascertains the slip velocities of spherical particles in foam fluids. Slip velocities were determined by writing a force balance for the particle in terms of physical parameters of the particle and foam, and solving the resulting equation for the slip velocity. He used laboratory data collected for various particle sizes and foam qualities to ascertain empirically particle drag coefficients. He derived two equations describing slip velocity results. One equation describes slip velocities in foams displaying Newtonian behavior while the second equation describes slip velocities in foam displaying Bingham plastic behavior. Abbott, in his conclusions, writes that slip velocity increases with increasing effective viscosity and allows this observation to be caused by increasing foam quality or decreasing shear rate. Also, the slip velocity of spherical particles in foam are similar in value to those of a moderate yield point drilling fluid.

Blauer (1974) presented an extension of Mitchell's data to larger-size tubular goods and to turbulent flow. Blauer found Reynold's numbers and Fanning friction factors could be calculated with effective foam viscosity, actual foam density, average velocity, and true pipe diameter.

In his conclusions, he writes that foam behaves as does a single-phase Bingham plastic fluid, and the friction losses may be determined as for a single-phase fluid using conventional Reynold's number and Moody's diagram.

Most solids have densities greater than those of the liquid in which they are suspended. Therefore, there is a tendency for solid material to settle. The rate of settling depends upon particle size, shape and density, concentration of particle, liquid density and viscosity, and velocity of the liquid which is influenced by the geometry of the confining vessel or pipe and the presence of other particles.

Blauer and Kohlhaas (1974) measured settling velocities of several common sized sand particles in static foam. They found settling velocity is a function of foam viscosity, interfacial tension between the gas and liquid phase, particle size, and bubble size. Their data show that settling velocities of particles in foams are much less than settling velocities in water or gelled water and that settling velocities of small-diameter particles are much less than predicted by Stoke's law. The difference becomes less as particle size becomes larger. Particles much smaller than bubble size are believed to be retained within the gas bubble and have no settling velocity.

Abbott (1974) shows slip velocity equations for both Newtonian and Bingham plastic fluid:

$$V_S = 0.069 N_R^{0.36} \sqrt{\frac{R_p g (\rho_p - \rho_f)}{\rho_f}} \quad \begin{array}{l} 0 < \Gamma < .54 \\ 50 < N_R < 200 \end{array}$$

and

$$V_S = \sqrt{\frac{0.144 N_R^6 R_p g (\rho_p - \rho_f)}{\rho_f} - \frac{1.33 \tau_y g C_D}{\rho_f}} \quad \begin{array}{l} 4.4 < N_R < 78 \\ .54 < \Gamma < .96 \end{array}$$

where

R_p = radius of spherical particle

ρ_p = density of the particle

ρ_f = density of the fluid

g = acceleration of gravity

V_S = particle slip velocity

τ_y = yield strength

N_R = Reynold's number's

C_D = Drag coefficient .

The above two equations show that slip velocities depend on the radius of the particle. Cement particles range between 4 and 28 microns and slip velocities calculated with the above two equations are very small when compared

with the main stream velocities. Therefore, the settling of cementitious particles within the flow tubes in any of the relevant experiments was considered negligible.

Foam cement can be defined as a dispersion of gas, most often nitrogen or air, in a cement slurry with small amounts of surfactant as a foaming agent. Emulsion as defined by Becher (1965) is:

"An emulsion is a heterogeneous system consisting of at least one immiscible liquid intimately dispersed in another in the form of droplets, whose diameters in general exceed 0.1 micron. Such systems possess a minimal stability, which may be accentuated by such additives as surface-active agents, finely-divided solids, etc."

The above two definitions, one of foam cement and the other of an emulsion, show a similarity and perhaps the theories of emulsions may in some applications be applied to foam cement. It is necessary to notice that foam cement is not an emulsion as defined by Becher because the dispersed phase is a gas and not a liquid.

Sherman (1955) listed the factors influencing emulsion rheological properties. They are:

1. External phase viscosity (μ_0)
2. Internal phase viscosity (μ_i)
3. Nature of the surface-active agent and the interfacial film formed.
4. Electrical force

5. Particle size distribution

6. Volume concentration of dispersed phase into the continuous phase.

The literature is conflicting on the importance of the viscosity of the internal phase in regard to the viscosity of an emulsion (μ) with most workers neglecting it. However, Taylor (1932) derived a theoretical equation relating viscosity of emulsion to the viscosity of the dispersed phase. His equation shown below is based on hydrodynamic theory and is an extension of Einstein's theory.

$$\mu = \mu_0 \left\{ 1 + 2.5 \Gamma \frac{\mu_i + \frac{2}{5}\mu_0}{\mu_i + \mu_0} \right\}$$

where

Γ = foam quality

μ_i = internal phase viscosity

μ_0 = external phase viscosity

μ = viscosity of foam .

The factor $\left[\frac{\mu_i + \frac{2}{5}\mu_0}{\mu_i + \mu_0} \right]$ accounts for an internal current within a particle of the dispersed phase which is within the continuous phase.

Reduction in particle size results in an increase in interfacial area and an increase in mutual interaction of the particles. Particle size and particle size distribution are important factors in describing the physical properties of emulsions.

Becher (1965) presented an equation derived by Schwarz and Bezemer which permits a better understanding of particle size distributions of emulsions (see Figure 1).

$$\frac{dn}{dx} \frac{100}{N} = \frac{100}{6} \frac{e^{x/X}}{\left(1 + \frac{a}{X} + \frac{a^2}{2X^2} + \frac{a^3}{6X^3}\right) x^5} \frac{a^4}{x^5} e^{-a/X}$$

where

n is the number of droplets of diameter x

N is the total number of droplets

X is the diameter of the largest drop present

a is constant and obtained graphically from the experimental data.

Richardson (1953) examined the viscosities of emulsions of differing bubble size distributions at several shear rates. He concluded that the apparent viscosity of emulsions having the same particle concentration and size distribution about a mean drop diameter is inversely proportional to this mean drop diameter.

Figure 2 shows some of Richardsons' data, where the apparent viscosities of four emulsions are a function of the imposed shear rate and bubble size distribution.

When the interaction among charged particles was taken into account, the following equation was derived by Smolvchowski (1903) to relate the viscosity to other properties of the suspension: The dielectric constant D , the electrokinetic potential (Zeta potential) ζ , the specific conductivity K and particle radius a .

$$\frac{\mu - \mu_0}{\mu_0} = 2.5 \Gamma \left[1 + \frac{1}{\mu_0 K a^2} \frac{(D\zeta)^2}{2\pi} \right]$$

Smolvchowski's equation, which is a modification of Einstein's equation, shows that a lyophobic bubble bearing an electric charge would show a viscosity exceeding that of a similar system of uncharged particles.

The relative viscosity increases irrespective of the sign of the charge and the electroviscous term

$$\left(\frac{1}{\mu_0 K a^2} \right) \left(\frac{D\zeta}{2\pi} \right)^2$$

is always positive.

Van der Waarden (1954) used the above equation in the analysis of his experimental work. He discussed the variable mentioned in the preceding section, and presented data which show that some emulsions exhibit a high increase in viscosity

if the percent by weight of the surface-active agent increases from 0 to 35 percent. He also wrote that the electrical effects can be reduced to approximately zero level by the addition of an electrolyte or by the selection of some types of ionic surface-active agent.

Lowering the surface tension of a liquid permits a greater dispersion of the gas bubbles and the manufacture of a more stable foam.

McBain, Ford, and Wilson (1937) classified three types of surface tension curves, as shown in Figure 3. Most soaps and detergents produce type III curves. McBain's data may be applied to foam, because it is a measurement of surface tensions of aqueous solutions in contact with air.

Fischer and Gans (1946) studied the range of surface tensions found in solutions of most surface-active materials, as shown in Figure 4. Their data were taken with the solutions in contact with air and thus can be applied to the foam.

It is known that for a spherical bubble the excess pressure across an interface is given by the following equation

$$\Delta P = \frac{2\sigma}{r}$$

where

ΔP = pressure differential, dynes per cm^2

σ = surface tension, dynes per cm

r = radius of the bubble, cm .

Thus, transfer of gas from a bubble to a larger adjacent bubble will occur through gas diffusion in the liquid phase. This has been discussed by Clark and Blackman (1948) and is one reason why the average bubble diameter of the foam should increase with time.

The mechanism of gas diffusion may be based on the preceding pressure equation in the following manner.

If the surface tension of a film is kept constant and the radii of two adjacent bubbles are not equal, then the pressure in the smaller bubble will exceed the pressure in the larger one and a pressure difference exists. If the liquid is not saturated, gas in the smaller bubble will diffuse into the liquid phase faster than gas in the larger bubble.

Once the liquid is saturated, gas escapes the smaller bubbles, diffuses through the liquid and is captured by the larger bubbles. Thus, there is a mass transfer of gas from the smaller to the larger bubble.

Liquid drainage also increases the spontaneous decomposition of foam through a reduction in the film thickness of a bubble. A temperature increase may cause further decomposition. Nevertheless, many foams are stable for long

periods of time. They can be stabilized by adding special chemicals, by decreasing the surface tension and hence the surface free energy, by ionic repulsion, and by increasing the liquid viscosity.

When a solid particle is attached to a bubble as shown in Figure 5, it reduces bubble coalescence and, in this manner, enhances foam stability.

Bikerman (1973) explains the mechanism of how solid particles become attached to bubbles:

"When the receding contact angle θ_r (in the liquid) is large, for instance, 60° (or over a radian), then the particle becomes attached to a bubble and rises with it because of buoyance. Figure 5 may help in understanding the mechanism of this effect. The solid particle is supposed to hang at the bottom of the bubble; every other position would be just as suitable but a little more difficult to draw. Surface tension of the liquid pulls at the solid along the three-phase line (in which gas, liquid, and solid meet). If the tangent to the gas liquid interface at this line forms an angle β with the vertical (upward), then force $L\gamma \cos \beta$ pulls the particle vertically up; L is the length of the three-phase line. When this force exceeds that of gravitation, the particle remains attached to the bubble.

The angle β depends on two other angles. One is the receding contact angle θ_R mentioned above. A receding, rather than the equilibrium or an advancing contact angle, is deciding because the particles are initially immersed in the liquid, and the air in the bubble has to displace some of the liquid from the solid surface. The other angle is that formed by the vertical and the solid surface at the three-phase line. If ψ is this (obtuse) angle,

then (see Figure 6) $\beta = \psi - \theta_R$. The value of θ_R is, to an extent, determined by the compositions of the solid and the liquid; in actual flotation processes θ_R is, to an extent, determined by the compositions of the solid and the liquid; in actual flotation processes θ_R is deliberately adjusted, whenever indicated, by addition of "collectors" which become absorbed on the particle and alter its wettability. The value of ψ cannot be predicted. It is seen, however, that β is smaller, that is $\cos \beta$ and the force $L\gamma \cos \beta$ are greater, when ψ decreases (for a given θ_R). This means that a particle is more likely to be immobilized in the interface when the three-phase line follows a nearly horizontal than a nearly vertical plane.

Consider, as an example, a particle of volume 0.001 cm^3 and specific gravity 2 g/cm^3 . In an aqueous medium the gravitational force on it is about 1 dyne. The force pulling it up is $L\gamma \cos \beta$. If $\gamma = 60 \text{ g/sec}^2$ and $\cos \beta = 0.83$ (corresponding to $\beta \approx 34$), then L needs to be only 0.02 cm long to achieve balance of forces. The length of the edge of a cube whose volume is 0.001 cm^3 is 0.1 cm , that is, much greater than this L .

Therefore, it is concluded that foam cement is less affected by drainage than regular foam used by other experimenters.

Summary of Previous Work and its Relation to This Work

1. Above an undefined critical shear rate the apparent viscosity of foam increases with increasing quality and it appears foam cement behaves in the same way.
2. Above a critical shear rate the viscosity of foam for constant quality becomes constant and is perhaps true for foam cement.
3. Foam behaves as does Bingham-plastic fluid and it is expected that foam cement also behaves as such.

4. The viscosity of foam cement may be described by Hatschek's formula as modified to describe the viscosity of air water foam.
5. Foam cement passing through a flow tube probably generates electrical potential as does air water foam.
6. The viscosity of foam cement should increase with decreasing shear rate or increasing flow tube diameter as does foam.
7. Boyle's law if properly modified may be applied to both foam and foam cement for estimating qualities at various pressures.
8. Cement particles which are smaller than the gas bubbles do not settle or have negligible settling velocities in static foam.
9. Settling of cement particles in foam flowing through flow tube is most likely negligible for many processes.
10. Gas dispersions may be compared with liquid dispersions; however, gas bubbles are more likely to change in size at a higher rate and result in an interfacial surface area decrease in a shorter time period.
11. Because of viscosity differences between a gas and liquid dispersed phase, a gas bubble is considered more deformable than a liquid droplet; thus coalescence and inversion rates may be in contrast.

12. Solubility differences between gas and immisible liquid in an aqueous phase could effect their stabilities.

13. Density and viscosity difference between a dispersed gas and liquid bubble will effect size and distribution of the bubble within the continuous phase.

CHAPTER II. THEORY

The internal structure of foam cement allows it to withstand shear stress up to a certain yield value. Any additional shear above this critical point will alter the internal structure and cause the fluid to flow. When the stress is lowered to a point below the critical yield value, flow may cease. When linearity in a shear stress-shear rate diagram exists above a yield stress, the fluid is commonly called a Bingham plastic fluid. Because the data acquired in this research in foam cement agree with the points in the above discussion, and foam cement shows an apparent viscosity that is a non-linear function of shear stress, the Power Law and Bingham Plastic Models have been chosen as suitable rheological models. A Newtonian fluid exhibits a direct proportionality between applied shear stress and shear rate if the pressure and temperature are held constant. This defining relationship becomes

$$\tau = \frac{\mu}{g_c} \left(-\frac{dv_r}{dr} \right)$$

where μ = the absolute viscosity of the fluid

$(-\frac{dv_r}{dr})$ = an expression of the shear rate for laminar flow within a circular tube.

All fluids which do not confirm to a direct proportionality between shear rate and shear stress are classified as non-Newtonian. Several non-Newtonian models are popular.

1. Bingham Plastic

This kind of fluid may be described by the following equation:

$$(\tau - \tau_y) = \frac{\mu_p}{g} \left(-\frac{dv_r}{dr}\right) \quad \tau > \tau_y$$

By plotting shear rate versus shear stress, the yield point (τ_y), will be the positive intercept on the shear stress axis and plastic viscosity (μ_p) is proportional to the constant slope of a line relating shear stress and shear rate. The Bingham plastic fluid will not deform continuously (or flow) until the applied shear stress τ exceeds a certain minimum value τ_y known as the yield point. When the yield point value has been exceeded, equal increments of additional shear stress will produce equal increments of shear rate in proportion to μ_p called the plastic viscosity. These two rheological parameters, plastic viscosity and yield point, specify the flow properties of a Bingham plastic fluid.

For all non-Newtonian fluids, apparent viscosity defined as a ratio of the shear stress to the shear rate, is not constant but varies with the applied shear stress. (The apparent viscosity μ_a can be obtained from the slope of a straight line drawn from the origin and terminating at some point on the flow curve whose position coincides with a given value of shear stress.)

2. Pseudo Plastic and Dilatant Fluid

These types of fluids do not have yield points but their apparent viscosity is a non-linear function of shear stress. The apparent viscosity of a pseudo-plastic fluid will decrease with increasing value of shear stress. Dilatant fluid displays rheological behavior opposite to that of pseudo-plastic, in that its apparent viscosity increases with increasing shear stress.

Other non-Newtonian fluids do not have a yield stress, and are characterized by non linearity of the shear stress-rate at low and high shear rate. The simplest representation of this type of fluid is given by the power law equation

$$\tau = K \left(\frac{-dv_r}{dr} \right)^n .$$

Values of n between zero and unity characterize pseudo plastic fluid whereas dilatant fluid has n values greater than unity. The exponent n is a quantitative index which may be used to

evaluate the degree of non-Newtonian behavior. The greater the difference between n and unity, whether smaller or larger, the more pronounced are the non-Newtonian characteristics of a given fluid. The coefficient K is related to the consistency of a fluid, the larger the value of K , the more resistant the fluid is to flow.

Because the experimental data of the foam cement agrees in many aspects with the Power Law and Bingham plastic models; these are the models chosen for this work. For isothermal steady state flow of fluid through a straight tube the pressure loss caused by friction may be theoretically related to the average flow rate within the tube if subjected to the following assumptions according to Rabinowitsch (1929).

- "1. There is no slippage at the wall, i.e., the velocity of the fluid contacting the pipe wall is zero.
2. All particles situated in a cylindrical shell of radius r and infinitesimal thickness dr travel as a group at a constant velocity v_r parallel to the axis of the pipe.
3. The shearing rate or velocity gradient produced at any point in the flow, as one shell of fluid slides past another, is a function only of the shear stress at that point."

Consider a concentric cylinder of fluid of radius r and length L inside a region of steady flow of fluid in a horizontal flow tube section of radius r_w as shown in Figure 7. The pressure differential Δp_f acting over the end area πr^2

tend to push the cylinder in the direction of the flow. While the fluid particles on the surface area $2\pi rL$ of the cylinder are being sheared past those particles immediately outside this surface and as a result, they experience a shear stress τ which opposes the motion of the cylinder. For steady state flow of fluid within the cylinder, these forces must cancel each other, or

$$(P_1 - P_2) \pi r^2 = \Delta P_f \pi r^2 = \tau (2\pi rL)$$

Therefore, the produced shear stress along the surface of the fluid cylinder is:

$$\tau = \frac{r}{2} \left(\frac{\Delta P_f}{L} \right) \quad (1)$$

The shear stress developed at the tube wall is

$$\tau_w = \frac{D \Delta P_f}{4L} \quad (2)$$

which is a measurable quantity. From equations (1) and (2), the shear stress distribution within the fluid can be obtained

$$\tau = \frac{2\tau_w}{D} r \quad (3)$$

or

$$d\tau = \frac{2\tau_w}{D} dr \quad (3a)$$

in which τ is a linear function with the radius r , as shown in Figure 7.

The shear rate, was assumed to be a function of the shear stress

$$\left(\frac{-dv_r}{dr}\right) = k\phi(\tau) \quad (4)$$

where k is a constant and $\phi(\tau)$ represent the function of shear stress τ . The negative sign appears in the above equation, because dv_r/dr is a negative quantity.

From equations (3) and (4)

$$dv_r = -\frac{kD}{2\tau_w} \phi(\tau) d\tau \quad (5)$$

By integrating the above equation from some point at radius r to the wall where $r = r_w$, the velocity distribution in the tube will be

$$\int_r^{r_w} dv_r = -\frac{kD}{2\tau_w} \int_{\tau}^{\tau_w} \phi(\tau) d\tau \quad \begin{array}{l} \text{at } r \text{ velocity} = v_r \\ \text{at } r = r_w \text{ velocity} = 0 \end{array}$$

$$v_r = \frac{kD}{2\tau_w} \int_{\tau}^{\tau_w} \phi(\tau) d\tau \quad (6)$$

The volumetric flow rate of the fluid through a cylindrical shell of radius r and thickness dr which is moving at a velocity v_r is given by

$$dq = 2v_r \pi r dr \quad (7)$$

from equations (3) and (3a)

$$2\pi r dr = \frac{\pi D^2}{2\tau_w^2} \tau d\tau \quad (7a)$$

Substituting equations (7a) and (6) into equation (7), the differential flow rate can be rewritten in terms of the shear stress τ

$$dq = \frac{\pi k D^3}{4\tau_w^3} \tau' \left[\int_{\tau}^{\tau_w} \phi(\tau') d\tau' \right] d\tau' \quad (8)$$

integrating the right side of equation (8) from $\tau = 0$ to $\tau = \tau_w$, will yield the total flow rate

$$q = \frac{\pi k D^3}{4\tau_w^3} \int_0^{\tau_w} \tau' \left[\int_{\tau}^{\tau_w} \phi(\tau') d\tau' \right] d\tau' \quad (9)$$

and

$$v = \frac{4q}{\pi D^2}$$

where v is the average velocity of the flow. Equation (9) can be rearranged into the following form

$$\frac{v}{D} = \frac{k}{\tau_w^3} \int_0^{\tau_w} \tau' \left[\int_{\tau}^{\tau_w} \phi(\tau') d\tau' \right] d\tau' \quad (10)$$

The general expression for laminar pipe flow can be obtained by integrating equation (10) by parts to give

$$\frac{v}{D} = \frac{k}{2\tau_w^3} \int_0^{\tau_w} \tau^2 \phi(\tau) d\tau \quad (11)$$

For Bingham plastic fluid

$$\begin{aligned}\phi(\tau) &= (\tau - \tau_y) && \text{for } \tau > \tau_y \\ \phi(\tau) &= 0 && \text{for } \tau \leq \tau_y\end{aligned}$$

and

$$k = g/\mu_p$$

By substituting these relations into equation (11), we obtain

$$\frac{v}{D} = \frac{g}{2\mu_p \tau_w^3} \left[\int_0^{\tau_y} \tau^2(0) d\tau + \int_{\tau_y}^{\tau_w} \tau^2(\tau - \tau_y) d\tau \right]$$

or

$$\frac{8v}{gD} = \frac{\tau_w}{\mu_p} \left[1 - \frac{4}{3} \left(\frac{\tau_y}{\tau_w} \right) + \frac{1}{3} \left(\frac{\tau_y}{\tau_w} \right)^4 \right] \quad (12)$$

when $\tau = \tau_y$ the term in the brackets becomes zero which means that the shear stress imposed on the fluid in contact with the wall must always exceed the yield point of the fluid in order to maintain flow. From equation (3) and Figure 7, which show the shear stress distribution, it is possible to see that even when $\tau_w > \tau_y$ there will always remain a central core of diameter $D[\tau_y/\tau_w]$ within which the stress is very much less than τ_y . The fluid within this core moves as a plug and only the fluid outside this core will flow in laminar flow.

Since the quantity $(\tau_y/\tau_w)^4$ is relatively small, the term $\frac{1}{3} \left(\frac{\tau_y}{\tau_w} \right)^4$ can be dropped from equation (12) to get the approximate expression

$$\frac{8v}{qD} = \frac{1}{\mu_p} [\tau_w - \frac{4}{3} \tau_y] \quad (13)$$

which is linear in τ_w and at $v = 0$ (the intercept) the value of $\tau_w = \frac{4}{3} \tau_y$.

The general expression for laminar tube flow is given by equation (11),

$$\frac{(2v)}{kD} \tau_w^3 = \int_0^{\tau_w} \tau^2 \phi(\tau) d\tau \quad (11)$$

when differentiated with respect to τ_w yields

$$\frac{(2v)}{kD} 3 \tau_w^2 + \tau_w^3 \frac{d(2v/kD)}{d\tau_w} = \tau_w^2 \phi(\tau_w),$$

which can be simplified by multiplying all terms by $\left(\frac{k}{\tau_w^2}\right)$ to obtain

$$3 \frac{(2v)}{D} + \tau_w \frac{d(2v/D)}{d\tau_w} = k \phi(\tau_w).$$

The shear rate (dv_r/dr) was assumed to be a function of shear stress represented by $k \phi(\tau)$, which appears in equation (4), only now it is evaluated at the value of shear stress developed at the tube wall, τ_w and it is represented by the shear rate at the tube wall denoted by $(-dv_r/dr)_w$. Replacing τ_w by $(D\Delta P_f/4L)$ and $k \phi(\tau_w)$ by its equivalent the last equation will become

$$\phi_w = \left(-\frac{dv_r}{dr_w}\right) = \frac{3}{4} \frac{(8v)}{D} + \frac{1}{4} \frac{(D\Delta P_f)}{4L} \frac{d(8v/D)}{d\left(\frac{D\Delta P_f}{4L}\right)} \quad (14)$$

which express the rate of the shear at the tube wall caused by applied shear stress, τ_w . Metzner and Reed (1955) modified the last term of equation (14) as follows:

$$\left(-\frac{dv_r}{dr}\right)_w = \frac{3}{4} \frac{(8v)}{D} + \frac{1}{4} \frac{(8v)}{D} \frac{d\left(\frac{8v}{D}\right) / \left(\frac{8v}{D}\right)}{d\left(\frac{D\Delta P_f}{4L}\right) / \left(\frac{D\Delta P_f}{4L}\right)}$$

recalling $d(\ln x) = dx/x$, the last equation can be written as

$$\left(-\frac{dv_r}{dr}\right)_w = \frac{3}{4} \frac{(8v)}{D} + \frac{1}{4} \frac{(8v)}{D} \frac{d \ln(8v/D)}{d \ln\left(\frac{D\Delta P_f}{4L}\right)} \quad (15)$$

by representing

$$n' = \frac{d \ln(D\Delta P_f/4L)}{d \ln(8v/D)} \quad (15a)$$

Metzner and Reed rearranged equation (15) to the following form

$$\left(-\frac{dv_r}{dr}\right)_w = \frac{3n' + 1}{4n'} \frac{(8v)}{D} \quad (16)$$

where n' can be evaluated from the slope of a logarithmic plot of viscometric data in the form of $(D\Delta P_f/4L)$ versus $(8v/D)$.

For fluid which obeys the "power-law" relationship between shear stress and shear rate, is

$$\tau = K \left(-\frac{dv_r}{dr}\right)^n \quad (17)$$

if one takes logarithms of equation (17) one obtains

$$\log \tau = \log K + n \log \left(-\frac{dv_r}{dr} \right). \quad (18)$$

Because in writing equation (17) n and K are assumed to be constant over at least a differential range of shear rates and stresses, differentiation of equation (18) gives, within this range

$$n = \frac{d(\log \tau)}{d[\log (-\frac{dv_r}{dr})]}. \quad (19)$$

Comparison of equations (15a) and (19) bring out distinctions between n and n' , n is the slope of logarithmic plot of shear stress τ vs the corresponding shear rate $(-dv_r/dr)$, while n' is the slope of logarithmic plot of shear stress at the wall τ_w vs $8v/D$. The shear rate at the wall, at any given value of the wall shear-stress, is not in general equal to $8v/D$, as inspection of equation (16) shows. Therefore, these latter plots from which n' is determined are not actually shear stress-shear rate curves and should not be termed such except for the special case of Newtonian behavior ($n' = 1.00$).

The shear stress τ_w at the wall of a tube is equal to $(D\Delta P_f/4L)$. As n' is the slope of the logarithmic τ_w vs $8v/D$ curve, the equation of the straight line which is the tangent to the curve at a chosen value of τ_w may be written as

$$\tau_w = \frac{D\Delta P_f}{4L} = K' \left(\frac{8v}{D}\right)^{n'}, \quad (20)$$

where K' corresponds to a particular value of shear stress, τ_w . If the slope of the logarithmic curve happens to be constant over a range of shear stress, equation (20) also represents the equation of this straight line. If the slope of the logarithmic τ_w vs $8v/D$ plots is not a straight line, it is necessary to evaluate n' and K' at the appropriate value of shear stress.

A comparison of equations (17) and (20) shows the practical importance of equation (20) over equation (17). Equation (20) is a direct relationship between the pressure drop ΔP_f and the flow rate (average velocity) of the fluid v in terms of tube dimensions and parameters K' and n' . On the other hand equations (17) and (19) relate shear stress only to shear rate, and not to flow rate. To obtain an equation for the average flow velocity equation (17) must be integrated twice, over the entire range of shear stresses encountered in a tube - i.e., from $\tau = 0$ to $\tau = \tau_w$. Unless n were constant over this range, this would entail multiple integrations.

The relationship between n' and n at any particular shear stress, may be derived as follows. Taking logarithms of equations (16) and differentiating, one obtains:

$$d[\log(-\frac{dv_r}{dr})_w] = d(\log \frac{8v}{D}) + d(\log \frac{3n' + 1}{4n'}),$$

division by $d(\log \tau_w)$ gives

$$\frac{d[\log(-dv_r/dr)]}{d(\log \tau_w)} = \frac{d(\log 8v/D)}{d(\log \tau_w)} + \frac{d(\log \frac{3n' + 1}{4n'})}{d(\log \tau_w)}.$$

Noting that the first two terms of this equation also appear in equations (15a) and (19), one may write

$$\frac{1}{n} = \frac{1}{n'} + \frac{d(\log \frac{3n' + 1}{4n'})}{d(\log \tau_w)}. \quad (22a)$$

As n' is understood to refer to a particular value of the shear stress, and it is irrelevant whether this occurred at the wall of a tube or elsewhere, subscript w may be dropped in equation 22a. Then rearrangement gives:

$$n = \frac{n'}{1 - \frac{1}{3n' + 1} \times \frac{dn'}{d(\log \tau)}} \quad (22b)$$

The derivative in equation (22b) represents the slope of plot of n' vs $\log \tau$. Thus, if n' does not vary with shear stress - i.e., if the initial $\log \tau_w \log 8v/D$ plot is essentially a straight line, the second term of the denominator is zero and n becomes identically equal to n' .

Blauer (1974) shows that effective foam viscosity, true foam density, pipe diameter, and average foam velocity may be used to calculate Reynold's numbers and the Fanning friction factor for foam. The Reynold's number and Fanning friction factor are

$$N_R = \frac{v_f D \rho_f}{\mu_e}$$

$$f = \frac{\Delta P D}{2L \rho_f v_f^2}$$

where v_f = foam velocity

D = inside diameter of tube

ρ_f = foam density

μ_e = effective foam viscosity

L = tube length

Since the power law and Bingham plastic models were chosen for foam cement in this study, the N_R and "f" are also calculatable with the fluid properties n' and K' . These equations which require standard oil industry dimensional units are

$$N_R = \frac{1.86 v^{2-n'} \rho_f}{K' (96/D)^{n'}} \quad (23)$$

and

$$f = 16/N_R$$

The relationship between the Fanning friction factor and Reynold's number in the transition and turbulent region for non-Newtonian fluids is

$$f = 0.00454 + 0.645 (N_R)^{-0.70} .$$

Hatschek(1911) presented a theory relating the viscosity of a liquid containing a suspension of undeformable spheres of small diameter to the viscosity of the solvent and the concentration of the particles in the liquid. This relationship is expressed thus:

$$\mu_f = \mu_1(1 + 4.5\Gamma)$$

where

μ_f = viscosity of foam

μ_1 = viscosity of the continuous phase

Γ = foam quality

Mitchell (1969) re-iterated the basic assumptions for the Hatschek linear theory, which are:

- 1) Stoke's law applies
- 2) Only spherical solid particles (non-deformable) are present.
- 3) These particles are equal in size and uniform in their distribution within the solvent.
- 4) The viscosities of the pure solvent, i.e., without particles, and the solvent containing the particles, are proportional to the power required to sustain equal velocities of the two fluids in a linear, horizontal displacement motion.

- 5) The fluid is considered not to have dilation motion."

Hatschek's flow theories are valid for calculating the viscosity of the foam for quality ranges between the value of 0 percent up to 74 percent.

Einstein's assumptions, as translated by Mitchell (1969), are:

- "1) Solid particles are suspended in a homogeneous fluid which will hereafter be referred to as the solvent.
- 2) The particles are always spherical, homogeneous, of equal size (volume), and cannot possess momentum (weightless).
- 3) The volume of the particles is large when compared with the volume of the molecules composing the solvent.
- 4) The volume of the particles is small when compared with the volume of any region of the fluid regardless of the size of the fluid region selected.
- 5) The spacing of the particles, which is constant, is sufficiently large so that they do not mutually interfere in their motion.
- 6) The motion of a particle does not affect any region of the fluid which is located at an infinite distance from its surface.

- 7) There is no relative motion between the surface of the sphere and fluid contacting its surface.
- 8) The fluid has viscous properties.
- 9) The fluid cannot possess momentum.
- 10) Hydrodynamic equations are used to determine the motion of the particles and the solvent.
- 11) All functions, regardless of the variable under consideration, within any region of the solvent, are continuous and linear functions, except at the surface of a particle or within the boundary of a particle.
- 12) The motion of the fluid is determined by the superposition of three principal directions of dilation for a fluid. The problem is solved for a three-dimensional expansion of the suspension."

Einstein's final equation is

$$\mu_f = \mu_f (1 + 2.5\Gamma)$$

His mathematical model is presented in Mitchell's doctoral thesis (1969).

Hatschek's and Einstein's theories do not apply directly to foam cement but the similarities of properties required in the theories and those observed or reasoned for foam cement invite comparison. The major discordance with Hatschek's non-linear theory is that foam cement solid particles are not readily deformable as Hatschek's theory requires. While in contrast Einstein's theory calls for solid spherical particles.

CHAPTER III. EXPERIMENTS AND APPARATUS

The experimental apparatus constructed to study the flow of foam cement is shown in Figure 8 which consists of the following:

1. Cement injection system,
2. Foaming agent injection system,
3. Air injection system,
4. Air measuring system,
5. Foam cement generation system,
6. Flow tube system,
7. Pressure measuring system,
8. Differential pressure measuring system, and
9. Temperature monitoring system.

The various systems are described as follows.

1. Cement Injection System

The cement injection system consists of a 2 gallon capacity cement mixer with a maximum pressure rating of 50 psig which was used to feed the cement to a variable flow rate, positive displacement plunger pump with a maximum pressure rating of 3000 psi. The pump may be fitted with

plungers of various sizes to obtain a wide selection of cement flow rates. The plunger sizes in this experiment were 1/4 inch and 3/8 inch.

Pump calibration was done by keeping the stroke length constant and changing the RPM. For error estimates in the pump flow rate the dial number versus flow rate was plotted on semi-log paper in order to get a linear relationships between the two parameters as shown in Figure 9. A maximum variation of 5.0 percent was found based on 95 percent confidence intervals using the "t" distribution.

2. Foaming Agent Injection System

A variable flow rate positive displacement gear pump is used to inject the foaming agent into the cement. A small tube coil attached just after the foaming agent pump serves as a mixer of the foaming agent and cement. The capacity of the foaming agent pump ranges from zero to 1 gallon/hour.

3. Air Injection System

The air injection system consists of a compressor with a maximum pressure rating of 3500 psig, storage tanks, and piping. The air storage cylinders served as a liquid and dust particle trap. The sand pack connected after the air cylinders acts as a filter to the air going into the system. The pressure gauge shown after the sand pack monitors the

pressure of the air flowing to the air measuring system. It was calibrated four times during the experiment with a dead weight tester.

4. Air Measuring System

This system consists of a replaceable plate orifice meter rated to 3500 psig and a water manometer rated to 3000 psi. Orifice plate hole diameters were 0.01 inch and 0.006 inch. The system was calibrated four times during the experiment with wet gas meters. An expected variation of 0.1 percent in the calibration curves for a 99 percent confidence interval using "t" distribution was found.

5. Foam Cement Generation System

The foam cement generation system consists of three foam cement generators and connections. Each generator is a 12-inch long stainless steel, 1/2-inch OD thick wall tube with 0.33-inch ID filled with thin stainless steel shavings. These shavings cause turbulence which generates the foam cement.

6. Flow Tube System

This system consists of a replaceable stainless steel capillary tube with dimensions as shown in Table 1. The inside diameter as obtained from the calibration test deviated from that in the manufacturer's specification by 2 percent. This calibrated inside diameter was used in flow calculations in this investigation.

The length of the flow tube is 8 ft. Such a long flow tube reduces end effects (pressure disturbances) normally associated with small diameter tubes.

7. Pressure Measuring Systems

The pressure at each end of the flow tube was monitored to ascertain the absolute pressure within the flow tube. This was done by observing the two gauges which were calibrated two times and regularly checked for accuracy. None of them were found to be within a detectable error.

8. Differential Pressure Measuring System

The differential pressure measuring system measures the pressure difference over the length of the tube. The system consists of:

- a. A 40.0 psi mercury manometer which is rated to a maximum absolute pressure of 3000 psig. The manometer is constructed of 3/16-inch outside-diameter plastic tubing.
- b. A differential pressure transducer with a capacity of 500 psid and 2000 psi absolute pressure. The transducer was calibrated with a dead weight tester and a calibrated pressure gauge. An expected variation of 0.5 percent was found in the calibration curve based on a 99 percent confidence interval using the "t" distribution. The manometer was used

when differential pressure was less than 40 psid and the transducer was used above 40 psid.

9. Temperature Monitoring System

The temperature of the system was monitored by using two thermometers attached to the sides of the capillary tube. The temperature variance was minimal throughout the experimental work.

Calibration

For the calibration purpose, several Newtonian liquids of different viscosity were flowed through the capillary tubes at a wide range of flow rate. The fluids used in this test are:

- a) pure water,
- b) mixtures of glycerine and water, and
- c) glycerin.

The properties of the calibration fluids are presented in Table 2.

The liquid viscosity was checked with a rotary viscometer before and after running the fluid through the tube.

From the theory and the experiment it is found that by plotting shear rate vs. shear stress for a Newtonian fluid on logarithmic coordinates a linear relation is obtained, with a slope equal to unity. The viscosity can, therefore, be obtained by dividing the shear rate into the shear stress of each data point.

Figure 10 shows the relation between shear rate and shear stress for the calibration fluids and it may be noted that linear relationships exist with a slope equal to unity. Figure 11 and Table 2 shows the degree of agreement between the data obtained by capillary tubes and rotary viscometer.

Having established that there is a significant linear relation between the two variables, it will be important to describe the variability of the data about the fitted line in terms of confidence limit placed about the line. Two types of confidence limit were computed. The first describing the variability of a point on the fitted line, and the second describing the variability of an individual observation Y_i for a given value of X_i . The general expression for confidence limits is

$$Y_i \pm t_{v, \alpha/2} [\text{var}]^{1/2}$$

where Y_i denoted the point on the fitted line corresponding to X_i , that is $Y_i = a + bX_i$, and $t_{v, \alpha/2}$ is the value of Students' "t" with $v(=n-2)$ degrees of freedom corresponding to the double-tailed probability level α and "var" is the appropriate variance. A probability level α (most probably 0.025) is used on the critical region size of both limits, there is a $(1-\alpha)$ or 95 percent probability that these limits enclosed the true value. According to the above discussion, the calibration of the pump, orifice, and differential pressure transducer was treated by using suitable probability level α for each item.

Experimental error has been estimated for the calculated values of both shear rate and shear stress. It was found to be ± 8 percent and ± 7.5 percent, respectively, which gives a maximum mean square error of 10 percent.

Technique

Before a group of data was taken, the system was checked for errors in calibration by flowing water through the capillary tube at several flow rates. If the data fell within the calibrated region, air and foaming agents were introduced into the system to generate regular foam and to check whether the foam generator was in good condition. The cement was introduced into the system. After the foam cement became homogeneous and stable, the cement and air flow rates were recorded, and at the same time the absolute pressure and differential pressures were measured.

The flow rates of the cement and air were taken from the calibration chart made for the pump and orifice. The succeeding test was performed by changing both air and cement flow rates, or by changing either the air or the cement flow rate in order to obtain different qualities and flow rates. The absolute and differential pressures and flow rates were recorded after equilibrium had been established.

The system was grounded to the earth to eliminate electrical streaming potentials by using the surface casing of a water well located adjacent to experimental equipment.

CHAPTER IV. RESULTS AND DISCUSSION

Figure 12 through 17 present the data recorded in this study as suggested by Mooney and others. The data are shown on a graph with logarithmic axes. The Y-axis represents the shear stress at the wall of the tube (psf), while the X-axis presents a value of $(8v/D)$ (sec^{-1}). The shear rate may be calculated with equation (14) or (16). These curves show that the apparent viscosity of foam cement which can be obtained from the slope of a straight line drawn from the origin and terminated at some point on the flow curve decreases with increasing shear rate. This agrees with the Bingham-plastic and power law models. The slopes of the curves (n' , flow index) approaches unity at the higher shear rates while yield points are evident at the lower values. Thus, the power law or Bingham plastic models again appear applicable.

Figure 20 through 25 show that the apparent viscosities of foam cement within various quality ranges are dependent upon the flow regime in which the foam exists. These curves show that foam cement has higher apparent viscosities at lower shear rate which is attributed to plug flow. This observation agrees with Marsden (1965) and Mitchell (1969).

Figures 18 and 19 present apparent viscosity data related to foam cement quality. A comparison of Figure 18 and 19 indicates that the apparent viscosity of foam cement depends on the diameter of the tube which is contrary to the findings of Mitchell (1969) and other but agrees with Fried (1961) and may be explained by the existence of plug flow.

Because the system was built of stainless steel and grounded to earth, the streaming potentials caused by the flow of foam cement through a tube are neglected.

Figure 26 depicts the yield points of foam cement versus quality and has a general configuration similar to that displayed by Mitchell (1969). The least square method was used for determining the coefficients of the following empirical equations which relate the yield point and the plastic viscosity of the Bingham model with foam cement quality:

$$\tau_y = 0.338964 - 1.754009\Gamma + 3.0568498\Gamma^2 \quad .35 < \Gamma < .65$$

$$\text{Variance} = 0.72142 \cdot 10^{-5} \quad 0 < \left(\frac{8v}{D}\right) < 5000$$

$$\text{Standard deviation} = 2.6869 \cdot 10^{-3}$$

$$\text{Maximum deviation} = 0.002659 \text{ psf}$$

$$\text{Maximum \% deviation} = 1.4$$

$$\mu_p = 13.00021 - 71.336573\Gamma + 367.12431\Gamma^2 - 257.9818\Gamma^3 \quad 0 < \Gamma < .65$$

$$\text{Variance} = 0.25169 \quad 0 < \left(\frac{8v}{D}\right) < 5000$$

Standard deviation = 0.50169

Maximum deviation = 0.5938 cp

Maximum % deviation = 1.5.

Figures 28 and 29 show the relation between the flow behavior index (n) and the consistency index (K) of the power law model, with foam cement quality. The least square method was used to find these parameters.

The empirical equations are:

$$n = 1.010037 - 0.3664368\Gamma + 0.6376808\Gamma^2 \quad .35 \leq \Gamma \leq .65$$

$$\text{Variance} = 0.969750 \cdot 10^{-8} \quad \left(\frac{8v}{D}\right) > 5000$$

$$\text{Standard deviation} = 9.84758 \cdot 10^{-5}$$

$$\text{Maximum deviation} = 0.0$$

$$\text{Maximum \% deviation} = 0.0$$

$$K = 0.00027123 - 0.00047757\Gamma + 0.0029789\Gamma^2 \quad 0 \leq \Gamma \leq .65$$

$$\text{Variance} = 0.15551 \cdot 10^{-9} \quad \left(\frac{8v}{D}\right) > 5000$$

$$\text{Standard deviation} = 1.24743 \cdot 10^{-5}$$

$$\text{Maximum deviation} = 0.000016171 \frac{\text{lb f, sec}}{\text{lb}^2}$$

$$\text{Maximum \% deviation} = 0.7.$$

Because no data were collected in the range of quality between zero to 30 percent, the following equation was obtained to define viscosity in this range by taking the equation of the straight line connecting the viscosity at the lowest quality with the base fluid viscosity

$$\mu_{fc} = \mu_c (1 + 0.95\Gamma). \quad 0 \leq \Gamma \leq .30$$

Einstein's and Hatschek's theoretical equations are

$$\mu_f = \mu_L (1 + 2.5\Gamma)$$

$$\mu_f = \mu_L (1 + 4.5\Gamma)$$

For the quality range above 30 percent, the method of least squares was also used to fit the theoretical equation of Hatschek's to this data. The non-linear Hatschek's equation is:

$$\mu_f = \mu_L \left[\frac{1}{(1 - \Gamma^{0.33})} \right]$$

and was linearized by substituting

$$X = \log \Gamma$$

$$Y = \log (1 - \mu_c/\mu_{fc})$$

The resulting equation ascertained with the method of least squares using 40 data points is:

$$\mu_{fc} = \mu_c \left(\frac{1}{1 - \Gamma^{1.036}} \right)$$

where μ_{fc} = foam cement viscosity

μ_c = cement viscosity

Variance of linearity between X and Y = 0.0023

Standard deviation of linearity between X and Y = 0.4795

Maximum deviation = 0.0469

Maximum % deviation = 10.4.

From the above discussion it was found that foam cement behaves almost the same way as air water foam. Einstein and Hatchek's theories were modified to predict the foam cement viscosity. It was also found that shear rate has an effect on the viscosity of foam cement which is true for air water foam.

Conclusions

1. The viscosity of foam cement increases as foam cement quality increases for each value of shear rate.
2. The viscosity of foam cement is dependent on both foam cement quality and shear rate for foam quality greater than 30 percent.
3. Air-cement-surfactant fluid can exist as a quasi-stable foam cement between foam cement qualities of zero and 70 percent.
4. Coalescence of foam cement is a slow process if the foam cement is quiescent in the environment in which it was created.
5. The yield point τ_y of foam cement is related to foam cement quality.
6. The flow behavior index (n) and consistency index (K) of foam cement are related to foam cement quality.
7. Foam cement can be mixed and pumped through a foam system consisting of tubes, valves, fittings, and orifices in the quality range of 0 percent to 70 percent and pressures to 1000 psia.

NOMENCLATURE

τ = shear stress, psf
 y = yield point, psf
 r = plastic viscosity cp
 v = average velocity, ft/sec
 a = apparent viscosity cp
 ρ = density
 ϕ = shear rate, sec^{-1}
 f = foam cement viscosity, cp
 c = base fluid viscosity, cp
 Γ = quality fraction
 p = pressure, psi
 q = flow rate
 v_s = slip velocity
 N_R = Reynold's number
 R_p = Particle radius
 P = differential pressure
 D = tube inside diameter, in.
 n' = flow index
 K' = consistency index
 f = Fanning friction factor

BIBLIOGRAPHY

1. Sibree, J.O., "The viscosity of froth", Trans. Farad. Soc. 30, 325 (1934). ✓
2. Penney, W.A., Blackman, M., "The mechanical properties of foam and the flow of foam through pipes", Ministry of Home Security (Britain), Note 282 (1943).
3. Grove, C.S., Jr., Wise, G.E. Jr., Marsh, W.C., Gray, J.B., "Viscosity of fire fighting foam", Ind. Eng. Chem., Volume 43 (1951), p. 112. ✓
4. Wise, G.E., Jr., "Fluid dynamics and other studies of mechanical fire fighting foam", Ph.D. Dissertation, Syracuse Univ., June 1951.
5. Fried, N.A., "The foam drive process for increasing the recovery of oil", U.S.G.M., Report of Investigation, No. 5866 (1961).
6. Marsden, S.S., Jr., Khan, W.A., "The flow of foam through short porous media and apparent viscosity measurements", Society of Petroleum Engineers Journal, Volume 237, March (1966) p. 17.
7. Marsden, S.S., Jr., Razon, S.H., "The streaming potential and the rheology of foam", Society of Petroleum Engineers Journal, Volume 7 (1967), p. 4.
8. Einstein, Albert, "Eine neue bestimmung der molekuldimensionen", Annaler der Physik, Volume 19, Ser. 4 (1906), p. 289.
9. Hatschek, Emil, "Die viskositat der dispersoide", Kelloid Z, Volume 7 (1910), p. 301.

10. Hatschek, Emil, "The general theory of viscosity of two-phase systems", The Faraday Society Trans., Volume 9, (1913-1915), p. 80.
- ✓ 11. Mitchell, B.J., "Viscosity of foam", Ph.D. Thesis, Univ. Okla., 1969.
12. Krug, Jack A., "Air and water requirement for foam drilling operations", Master of Science Thesis, Colorado School of Mines, 1971.
- ✓ 13. Krug, Jack A., Mitchell, B.J., "Charts help find volume, pressure needed for foam drilling", Oil and Gas Jour., Feb 7, 1972, p. 61-64.
14. Abbott, W.A., "An analysis of slip velocities of spherical particles in foam drilling fluid", Master of Science Thesis, Colorado School of Mines, 1974. ✓
- ✓ 15. Blauer, R.E., Mitchell, B.J., and Kohlhaas, C.A., "Determination of laminar, turbulent, and transitional foam flow friction losses in pipes", Paper SPE 4885 presented at SPE-AIME 44th Annual California Regional Meeting, San Francisco, California, April 4-5, 1974.
16. Blauer, R.E., Kohlhaas, C.A., "Formation fracturing with foam", Paper SPE 5003 presented at SPE-AIME 49th Annual Fall Meeting, Houston, Texas, Oct. 6-9, 1974.
17. Becher, Paul, Emulsions: Theory and practice, Reinhold Publishing Company (1957). ✓
18. Sherman, P., "Factors influencing emulsion viscosity and stability", Research (London), Volume 8, (1955), p. 396. ✓
19. Taylor, G.E., "The viscosity of a fluid containing small drops of another fluid", Proceedings of the Royal Society (London) Volume A138 (1932), p. 41.
20. Richardson, E.G., "The flow of emulsion II", J. Colloid Sci., 8, 367 (1953).
21. Smoluchowski, M.V., "Polska akademia umiejetnosic", Bull. Acad. Science Cracovie, (1903), p. 182.

22. Van der Waarden, J., "Viscosity and electroviscous effect of emulsions", *Journal Colloid Science*, Volume 9 (1954), p. 215.
23. McBain, J.W., Ford, T.F., Wilson, D.A., "Neue Methoden zum Studium der Oberflächen gewöhnlicher Lösungen", *Kolloid-Z.*, Volume 78, (1937), p. 1.
24. Fischer, E.K., and Gans, D.M., "Surface active agents at interfaces", *Ann. N.Y. Acad. Sci.*, Volume 46, (1946) pp. 371-406. ✓
25. Clark, N.O., Blackman, M., "The degree of dispersion of the gas phase in foam", *Trans. Farad. Soc.*, 44.1 (1948).
26. Bikerman, J.J., "Foam", Springer-Verlag, New York, 1973.
27. Rabinowitsch, R., "Über die Viskosität und Elastizität von Solen", *Zts. Phys. Chem.*, A 145, 1 (1929).
28. Metzner, A.B., Reed, J.C., "Flow of non-Newtonian fluid correlation of the laminar, transition and turbulent-flow regions", *Journal of American Institute Chemical Engineers*, 1, 434 (1955).
29. Metzner, A.B., "Non-Newtonian fluid flow", *Industrial and Engineering Chemistry*, Volume 49, No. 9, 1429 (1957).
30. Slagle, K.A., "Rheological design of cementing operations", *Journal of Petroleum Technology*, 323, March 1962. ✓
31. Marsden, S.S., Jr., Eerligh, J.J.P., Albrecht, R.A., David A., "Use of foam in petroleum operations", presented at the 7th World Petroleum Congress, Mexico City, Mexico, April 3-23, 1967. ✓
32. Richardson, E.G., "The formation and flow of emulsion", *J. Colloid Sci.*, 5, 404 (1950). ✓
33. Mooney, M., "Explicit formulas for slip and fluidity", *J. of Rheology* 2, 210 (1931).
34. Nawab, M.A., Mason, S.A., "The viscosity of dilute emulsions", *The Farad. Soc. Trans.*, Vol. 54 (1958), p. 1712.

35. Broughton, G., and Squires, L., "The viscosity of oil-water-emulsions", J. Physical Chemistry, Vol. 42 (1938), p. 253.
36. Wladimir, P., and Frederick, H.G., "The capillary experiment in rheology", Trans., Soc. Rheo., Vol. II, 263-284 (1958).

TABLE 1

Dimension of Flow Tube

<u>Tube No.</u>	<u>Manufacture I.D. Inches</u>	<u>Calculated I.D. Inches</u>	<u>Percent Reduction</u>	<u>Length of Effective Tube Ft.</u>
1	0.093	0.091	2.15	8
2	0.132	0.130	1.515	8

TABLE 2

Flow Tube Calibration

<u>Fluid Type</u>	<u>Viscosity Measured by Flow Tube cp</u>	<u>Viscosity Measured by Rotary Viscometer cp</u>
Glycerine	574.75	615.0
Glycerine and water mixture #1	5.0	6.0
Glycerine and water mixture #2	9.898	15.5
Glycerine and water mixture #3	36.65	41.0
Glycerine and water mixture #4	62.86	70.0
Glycerine and water mixture #5	158.08	170.0
Water	0.85	0.9

TABLE 3

Fluid Type: Water

<u>Flow Rate</u> <u>Cu. Ft/Sec.</u>	<u>Pressure</u> <u>Drop</u> <u>ΔP psi</u>	<u>Shear</u> <u>Rate</u> <u>Sec⁻¹</u>	<u>Shear</u> <u>Stress</u> <u>psf</u>
3.1993 x 10 ⁻⁵	15.029	7335.5	0.2395
2.8212 x 10 ⁻⁵	13.064	6468.76	0.2082
2.4926 x 10 ⁻⁵	11.173	5715.27	0.1780
2.0620 x 10 ⁻⁵	9.037	4728.05	0.1440
1.6379 x 10 ⁻⁵	7.244	3755.60	0.1154
1.0237 x 10 ⁻⁵	4.322	2347.31	0.0688

Fluid Type: Glycerine

3.7585 x 10 ⁻⁶	29.960	78.819	1.0448
2.6800 x 10 ⁻⁶	22.053	56.227	0.7690
2.0216 x 10 ⁻⁶	17.804	42.394	0.6209
1.4533 x 10 ⁻⁶	12.671	30,478	0.4419
0.9039 x 10 ⁻⁶	07.023	19.009	0.2449

TABLE 3 (continued)

Fluid Type: Glycerine and Water Mixture #1

<u>Flow Rate</u> <u>Cu. Ft./Sec.</u>	<u>Pressure</u> <u>Drop</u> <u>ΔP psi</u>	<u>Shear</u> <u>Rate</u> <u>Sec^{-1}</u>	<u>Shear</u> <u>Stress</u> <u>psf</u>
2.9698×10^{-5}	38.752	6809.22	0.6176
2.6418×10^{-5}	34.184	6057.37	0.5448
2.2552×10^{-5}	29.076	5171.96	0.4634
1.9879×10^{-5}	25.613	4557.96	0.4082
1.6381×10^{-5}	21.414	3756.01	0.3412
1.2625×10^{-5}	17.043	2894.88	0.2716
0.8990×10^{-5}	13.138	2061.38	0.2093

Fluid Type: Glycerine and Water Mixture #2

1.2701×10^{-5}	37.37	2912.07	0.5956
1.0906×10^{-5}	31.77	2500.51	0.5064
0.9372×10^{-5}	26.81	2149.04	0.4274
0.7599×10^{-5}	21.97	1742.47	0.3502
0.6453×10^{-5}	18.81	1479.73	0.2998
0.4405×10^{-5}	13.55	1010.01	0.2160
0.2641×10^{-5}	09.08	0605.70	0.1448

TABLE 3 (continued)

Fluid Type: Glycerine and Water Mixture #3

<u>Flow Rate</u> <u>Cu. Ft/Sec.</u>	<u>Pressure</u> <u>Drop</u> <u>ΔP psi</u>	<u>Shear</u> <u>Rate</u> <u>Sec.⁻¹</u>	<u>Shear</u> <u>Stress</u> <u>psf</u>
7.8814×10^{-5}	37.84	1724.59	1.3198
6.9628×10^{-5}	33.10	1523.61	1.1545
6.1121×10^{-5}	28.53	1337.39	0.9952
5.3400×10^{-5}	25.19	1168.51	0.8787
4.5633×10^{-5}	21.83	998.56	0.7613
3.8415×10^{-5}	18.78	840.629	0.6551
3.3123×10^{-5}	16.23	724.82	0.5661

Fluid Type: Glycerine and Water Mixture #4

4.4772×10^{-5}	39.16	979.71	1.366
3.9634×10^{-5}	34.20	867.28	1.193
3.5893×10^{-5}	30.99	785.42	1.0808
3.0740×10^{-5}	26.57	672.66	0.9266
2.5074×10^{-5}	22.17	548.67	0.7733
1.8772×10^{-5}	17.19	410.77	0.5995

Fluid Type: Glycerine and Water Mixture #5

1.6601×10^{-5}	34.82	363.27	1.214
1.4803×10^{-5}	29.71	323.92	1.036
1.2212×10^{-5}	25.39	267.14	0.885
0.926×10^{-5}	19.49	202.62	0.680

TABLE 4

Foam Cement Flow Data

Foam Cement Quality: $0.3 < \Gamma < 0.4$

<u>Quality Fraction</u>	<u>Velocity Ft/Sec.</u>	<u>Pressure Drop Δp psi</u>	<u>Shear Rate $(8v/D)$ Sec^{-1}</u>	<u>Shear Stress $(D\Delta P/4L)$ psf</u>	<u>Viscosity cp.</u>
0.3970	4.8688	31.87	3541.0	1.578	21.33
0.4000	7.9250	105.29	8181.4	3.672	21.49
0.3560	3.3194	29.74	2414.1	1.472	29.20
0.3680	3.3846	29.52	2461.6	1.461	28.43
0.3931	9.5216	31.67	2561.2	1.578	29.50
0.3907	3.5070	31.87	2550.9	1.577	29.62
0.3028	3.6650	27.44	2229.3	1.359	29.18
0.3749	3.4190	26.55	2486.6	1.314	25.32
0.3692	3.3880	25.30	2464.0	1.252	24.34
0.3980	3.5510	31.60	2582.2	1.564	29.01
0.3823	3.4590	30.62	2516.2	1.516	28.85
0.3380	2.5710	16.15	1668.0	0.897	25.75
0.3590	2.6540	18.74	1721.5	1.041	28.94
0.3844	2.7610	22.09	1791.5	1.226	32.78
0.3721	2.7070	19.93	1756.3	1.106	30.16
0.3816	2.7490	22.30	1783.3	1.238	33.25
0.3854	2.7660	22.36	1794.2	1.241	33.13
0.3281	4.3640	31.68	3174.0	1.568	23.66
0.3201	4.3140	29.72	3136.8	1.471	22.46
0.3271	4.3578	30.04	3169.0	1.487	22.47

TABLE 4 (continued)

<u>Quality Fraction</u>	<u>Velocity Ft/Sec.</u>	<u>Pressure Drop ΔP psi</u>	<u>Shear Rate $(8v/D)$; Sec^{-1}</u>	<u>Shear Stress $(D\Delta P/4L)$ psf</u>	<u>Viscosity cp.</u>
3.4486	4.501	33.48	3274.0	1.657	24.24
0.3436	4.467	30.51	3248.9	1.510	22.26
0.3390	4.440	28.57	3230.4	1.414	20.97
0.3152	4.282	31.17	3114.4	1.543	23.73
0.3161	4.287	30.89	3118.1	1.529	23.49
0.3320	4.391	33.39	3193.7	1.653	24.79
0.3443	4.472	34.01	3252.2	1.684	24.79
0.3879	5.131	39.42	3732.1	1.951	24.04
0.3836	5.095	36.57	3706.0	0.811	23.39
0.3747	5.023	35.76	36.528	1.770	23.21
0.3570	0.187	98.55	9483.7	3.437	16.35
0.3550	9.158	98.61	9453.0	3.439	17.42
0.3521	9.118	98.63	0412.2	3.439	17.50
0.3410	8.964	93.72	9253.4	3.268	16.91
0.3470	9.052	96.65	9344.2	3.370	17.27
0.3487	9.084	94.73	9376.7	3.303	16.87
0.3473	9.051	103.30	9343.0	3.603	18.46
0.3490	9.075	104.20	9367.0	3.634	18.58
0.3473	9.050	104.15	9342.0	3.632	18.62
0.3822	9.562	111.72	9871.0	3.896	18.90
0.3846	8.517	104.58	8792.2	3.647	19.86

TABLE 4 (continued)

<u>Quality Fraction</u>	<u>Velocity Ft/Sec.</u>	<u>Pressure Drop ΔP psi</u>	<u>Shear Rate $(8v/D)$; Sec^{-1}</u>	<u>Shear Stress $(D\Delta P/4L)$ psf</u>	<u>Viscosity cp.</u>
0.3837	8.505	105.00	8779.5	3.6619	19.97
0.3779	8.426	100.50	8698.0	3.5048	19.29
0.3613	8.206	93.68	8470.9	3.2672	18.47
0.3900	7.747	96.17	7997.3	3.3541	20.08
0.3990	7.792	94.91	8043.9	3.3100	19.70
0.3772	7.515	86.25	7757.0	3.0082	18.57

TABLE 5

Foam Cement Flow Data

Foam Cement Quality: $0.40 < \Gamma < 0.45$

<u>Quality Fraction</u>	<u>Velocity Ft/Sec.</u>	<u>Pressure Drop ΔP psi</u>	<u>Shear Rate $(8V/D)$ Sec^{-1}</u>	<u>Shear Stress $(D\Delta P/4L)$ psf</u>	<u>Viscosity cp.</u>
0.4300	3.1630	33.01	2300.3	1.6338	34.01
0.4280	3.7406	36.70	2720.4	1.8166	31.984
0.4296	8.204	110.26	8469.0	3.8452	21.746
0.4134	7.9775	108.76	8234.9	3.7931	22.060
0.4117	7.9544	103.80	8211.0	3.6201	21.116
0.4559	3.9255	45.87	2854.9	2.2708	38.090
0.4410	3.8232	39.53	2780.5	1.9571	33.710
0.4244	3.7130	36.56	2700.5	1.8101	32.103
0.4300	4.6638	93.76	4814.2	3.2700	32.532
0.4530	5.701	132.76	5885.5	3.6300	37.670
0.4089	3.616	34.55	2629.8	1.7104	31.150
0.4240	3.129	31.28	2276.1	1.5487	32.58
0.4440	3.244	34.82	2359.4	1.723	34.99
0.4450	3.8546	41.25	2803.3	2.042	34.88
0.4190	3.6837	35.18	2679.0	1.741	31.13
0.4260	3.7270	35.58	2710.9	1.761	31.11
0.4290	3.744	34.73	2723.6	1.719	30.23
0.4500	3.891	42.23	2830.3	2.090	35.37
0.4200	3.685	33.52	2680.3	1.6596	29.65

TABLE 5 (continued)

<u>Quality Fraction</u>	<u>Velocity Ft/Sec.</u>	<u>Pressure Drop ΔP psi</u>	<u>Shear Rate $(8v/D)$ Sec⁻¹</u>	<u>Shear Stress $(D\Delta P/4L)$ psf</u>	<u>Viscosity cp.</u>
0.427	3.732	34.50	2714.6	1.708	30.14
0.407	3.660	34.28	2622.5	1.697	30.98
0.419	3.683	34.77	2678.9	1.721	30.78
0.425	3.719	36.65	2704.7	1.814	32.13
0.401	2.840	22.36	1842.6	1.241	32.26
0.422	4.029	36.73	2930.3	1.818	29.72
0.442	4.168	41.47	3031.7	2.052	32.43
0.409	3.932	34.42	2849.8	1.703	28.53
0.410	3.947	35.98	2870.9	1.781	29.71
0.423	4.033	38.08	2933.2	1.884	30.77
0.423	40.35	37.27	2934.8	1.845	30.11
0.414	3.973	37.23	2889.7	1.842	30.54
0.420	4.007	37.85	2814.6	1.874	30.79
0.400	4.336	40.13	3153.6	1.986	30.17
0.409	3.939	35.75	2864.9	1.769	29.59
0.415	3.975	37.14	2891.5	1.838	30.45
0.409	4.407	41.72	3205.5	2.065	30.86
0.439	4.145	41.34	3015.1	2.046	32.50
0.401	4.350	44.42	3163.7	2.198	33.28
0.432	4.097	30.31	2979.8	1.500	24.11

TABLE 5 (continued)

<u>Quality Fraction</u>	<u>Velocity Ft/Sec.</u>	<u>Pressure Drop ΔP psi</u>	<u>Shear Rate $(8V/D)$ Sec^{-1}</u>	<u>Shear Stress $(D\Delta P/4L)$ psf</u>	<u>Viscosity cp.</u>
0.414	4.439	41.87	3228.4	2.072	30.75
0.407	4.384	40.13	3188.7	1.986	29.83
0.418	4.471	39.42	3251.9	1.951	28.74
0.405	4.373	42.36	3180.3	2.097	31.58
0.440	5.236	48.52	3808.8	2.402	30.21
0.404	4.915	33.92	3575.0	1.680	22.50
0.415	4.440	39.69	3231.0	1.965	29.12
0.421	5.064	36.19	3682.6	1.792	23.30
0.400	4.339	39.37	3156.2	1.948	29.57
0.429	4.555	43.84	3313.4	2.170	31.37
0.417	5.032	34.46	3660.0	1.706	22.32
0.444	6.535	87.14	6746.2	3.039	21.57
0.424	5.095	36.56	3705.0	1.809	21.57
0.423	9.085	99.40	9377.6	3.466	17.70
0.447	6.572	87.91	6784.6	3.066	21.64
0.429	7.540	97.41	7784.0	3.397	20.90
0.435	3.789	36.96	2755.7	1.830	31.80

TABLE 6

Foam Cement Flow Data

Foam Cement Quality: $0.45 < \Gamma < 0.50$

<u>Quality Fraction</u>	<u>Velocity Ft/Sec</u>	<u>Pressure Drop ΔP psi</u>	<u>Shear Rate $(8v/D)$ Sec⁻¹</u>	<u>Shear Stress $(D\Delta P/4L)$ psf</u>	<u>Velocity cp.</u>
0.4758	4.077	46.42	2965.3	2.298	37.12
0.4761	4.079	45.35	2867.1	2.245	36.24
0.4994	7.255	111.2	7489.2	3.880	24.81
0.4990	7.255	111.2	7489.9	3.880	24.81
0.4840	4.146	49.30	3015.5	2.440	38.76
0.4530	3.909	44.34	2843.3	2.194	36.97
0.4920	7.150	103.62	7381.5	3.613	23.44
0.4970	4.249	51.96	3090.7	2.572	39.86
0.4810	2.979	34.39	2166.9	1.702	37.62
0.4646	3.992	44.52	2903.5	2.204	36.36
0.4880	4.174	49.02	3036.1	2.426	38.27
0.4870	4.167	55.14	3030.2	2.729	43.14
0.4650	3.998	36.93	2907.7	1.828	30.11
0.4679	3.388	37.52	2464.2	1.858	36.10
0.4746	8.194	144.30	8459.3	5.032	28.49
0.5000	3.612	40.62	2626.9	2.010	36.60
0.4710	3.408	39.34	2478.7	1.947	37.63
0.4720	3.416	41.79	2485.0	2.069	39.87
0.4930	3.558	35.75	2587.8	1.769	32.75

TABLE 6 (continued)

<u>Quality Fraction</u>	<u>Velocity Ft/Sec.</u>	<u>Pressure Drop ΔP psi</u>	<u>Shear Rate (8v/D) Sec⁻¹</u>	<u>Shear Stress (DΔP/4L) psf</u>	<u>Velocity cp.</u>
0.495	3.57	39.39	2598.7	1.949	35.93
0.491	3.54	41.35	2577.5	2.047	38.03
0.476	3.445	37.13	2506.0	1.838	35.12
0.495	3.576	42.38	2600.9	2.098	38.63
0.475	3.433	37.13	2497.1	1.838	35.25
0.480	3.469	39.60	2523.5	1.960	37.20
0.505	4.322	52.41	3143.7	2.594	39.53
0.489	4.187	48.57	3045.2	2.404	37.81
0.496	4.241	47.05	3084.6	2.329	36.16
0.467	3.385	37.50	2462.4	1.856	36.10
0.486	3.507	40.58	2551.0	2.008	37.71
0.496	3.579	43.30	2603.3	2.143	39.43
0.497	3.588	43.57	2609.9	2.157	39.58
0.455	2.635	23.75	1709.4	1.315	36.86
0.500	2.879	30.68	1868.1	1.703	43.66
0.454	4.264	45.67	3101.7	2.260	34.91
0.471	4.400	48.39	3200.6	2.395	35.84
0.484	4.513	51.99	3282.6	2.573	37.55
0.498	4.642	53.92	3368.9	2.669	37.95
0.503	4.673	56.52	3399.2	2.797	39.42
0.469	4.382	47.01	3187.1	2.327	34.97

TABLE 6 (continued)

<u>Quality Fraction</u>	<u>Velocity Ft/Sec.</u>	<u>Pressure Drop ΔP psi</u>	<u>Shear Rate (8v/D) Sec⁻¹</u>	<u>Shear Stress (DΔP/4L) psf</u>	<u>Velocity cps.</u>
0.501	6.304	56.78	4584.9	2.811	29.36
0.486	7.075	91.16	7303.9	3.179	20.85
0.494	7.176	103.30	7408.3	3.602	23.29
0.488	7.095	98.62	7324.8	3.439	22.49
0.467	6.816	90.98	7035.9	3.173	21.60
0.498	4.632	53.92	3368.9	2.669	37.95
0.502	4.673	56.52	3399.2	2.797	39.42
0.469	4.382	47.01	3187.1	2.327	34.97
0.501	6.304	56.78	4584.9	2.811	29.36
0.486	7.075	91.16	7030.9	3.179	20.85
0.494	7.176	103.30	7408.3	3.602	23.29
0.488	7.095	98.62	7324.8	3.439	22.49
0.467	6.816	90.98	7035.9	3.173	21.60
0.483	7.035	98.53	7262.7	3.436	22.66
0.491	7.141	101.12	7371.7	3.526	22.91
0.473	6.901	97.24	7123.7	3.391	22.80
0.482	7.011	102.55	7237.5	3.576	23.66
0.473	6.895	88.75	7117.9	3.095	20.82
0.484	7.040	99.20	7267.5	3.459	22.80
0.478	6.967	101.97	7192.3	3.556	23.68
0.4931	7.164	108.22	7395.2	3.774	24.44

TABLE 7

Foam Cement Flow Data

Foam Cement Quality: $0.50 < \Gamma < 0.55$

<u>Quality Fraction</u>	<u>Velocity Ft/Sec.</u>	<u>Pressure Drop ΔP psi</u>	<u>Shear Rate $(8v/D)$ Sec⁻¹</u>	<u>Shear Stress $(D\Delta P/4L)$ psf</u>	<u>Velocity cps</u>
0.5031	3.627	42.19	2638.4	2.0884	37.91
0.5204	4.456	57.50	3240.9	2.8465	42.06
0.5426	3.380	48.79	2458.6	2.4152	47.05
0.5434	3.947	56.80	2871.2	2.8120	46.90
0.5117	4.376	54.35	3183.2	2.6900	40.48
0.5140	4.400	54.47	3200.1	2.6960	40.35
0.5100	4.315	54.17	3138.6	2.6820	40.92
0.5500	4.062	59.04	2954.5	2.9220	47.38
0.5400	3.936	55.54	2862.6	2.7490	46.00
0.5110	4.370	56.80	3181.7	2.8110	42.32
0.5000	4.278	51.65	3111.6	2.5560	39.35
0.5440	3.959	56.80	2879.5	2.8120	46.77
0.5000	4.277	53.14	3111.2	2.6306	40.49
0.5550	4.044	60.22	2948.6	2.9812	48.42
0.5540	4.049	59.07	2945.1	2.9240	47.55
0.5565	5.993	119.11	6187.0	4.1538	32.15
0.5400	5.779	113.16	5966.0	3.9460	31.68

TABLE 7 (continued)

<u>Quality Fraction</u>	<u>Velocity Ft/Sec.</u>	<u>Pressure Drop ΔP psi</u>	<u>Shear Rate $(8v/D)$ Sec^{-1}</u>	<u>Shear Stress $(D\Delta P/4L)$ psf</u>	<u>Velocity cp.</u>
0.550	4.037	59.57	2936.1	2.949	48.10
0.524	6.547	137.9	6758.5	4.809	34.08
0.509	6.349	122.94	6554.6	4.287	31.32
0.523	6.531	137.50	6742.0	4.796	34.07
0.528	7.707	137.87	7956.5	4.808	28.94
0.548	6.905	142.88	7127.9	4.982	33.48
0.550	7.009	142.44	7236.0	4.967	32.88
0.509	7.402	132.5	7641.4	4.623	28.97
0.550	8.227	158.25	8492.3	5.519	31.12
0.541	5.797	98.23	5984.2	3.425	27.42
0.531	7.746	145.48	7996.3	5.074	30.39
0.558	8.219	159.48	8484.5	5.561	31.39
0.520	7.558	138.51	7802.2	4.830	29.65
0.550	3.434	48.87	2498.0	2.419	46.38
0.537	3.339	47.54	2428.7	2.353	46.41
0.540	3.365	50.68	2447.5	2.509	49.10
0.541	3.370	48.96	2451.2	2.423	47.36
0.537	3.345	48.57	2432.7	2.404	47.34
0.550	3.435	50.44	2498.8	2.496	47.85
0.543	3.383	47.29	2460.6	2.341	45.57

TABLE 7 (continued)

<u>Quality Fraction</u>	<u>Velocity Ft/Sec.</u>	<u>Pressure Drop ΔP psi</u>	<u>Shear Rate $(8v/D)$ Sec⁻¹</u>	<u>Shear Stress $(D\Delta P/4L)$ psf</u>	<u>Velocity c_p</u>
0.534	3.322	48.42	2416.1	2.397	47.52
0.548	3.426	49.60	2491.9	2.455	47.19
0.548	3.424	53.88	2490.2	2.667	51.29
0.510	4.389	50.40	3192.6	2.494	38.00
0.540	3.412	50.19	2481.5	2.464	48.00
0.510	3.689	45.54	2683.4	2.254	40.23

TABLE 8

Foam Cement Flow Data

Foam Cement Quality: $0.55 < \Gamma < 0.60$

<u>Quality Fraction</u>	<u>Velocity Ft/Sec</u>	<u>Pressure Drop ΔP psi</u>	<u>Shear Rate $(8v/D)$ Sec⁻¹</u>	<u>Shear Stress $(D\Delta P/4L)$ psf</u>	<u>Viscosity cp.</u>
0.597	3.843	59.41	2794.9	2.940	50.39
0.563	3.539	54.29	2574.2	2.687	50.09
0.560	3.545	54.30	2578.6	2.688	49.92
0.590	3.826	59.32	2782.6	2.936	50.54
0.570	3.630	59.02	2640.3	2.922	53.00
0.560	3.579	56.75	2603.4	2.809	51.68
0.550	4.800	66.73	3591.3	3.303	45.32
0.555	4.050	58.91	2948.6	2.916	47.37
0.560	4.100	60.71	2982.2	3.005	48.27
0.600	3.950	61.08	2873.4	3.023	50.39
0.560	4.100	59.03	2982.4	2.922	46.93
0.566	4.150	60.01	3021.2	2.970	47.09
0.557	4.076	59.11	2964.4	2.926	47.28
0.578	4.279	63.99	3112.1	3.167	48.75
0.575	4.243	63.85	3086.0	3.161	49.05
0.561	4.112	61.54	2990.7	3.046	48.78
0.576	4.254	63.90	3094.3	3.163	48.96
0.571	4.209	63.50	3061.7	3.143	49.17

TABLE 8 (continued)

<u>Quality Fraction</u>	<u>Velocity Ft/Sec</u>	<u>Pressure Drop ΔP psi</u>	<u>Shear Rate $(8v/D)$ sec^{-1}</u>	<u>Shear Stress, $(D\Delta P/4L)$ psf</u>	<u>Viscosity</u>
0.584	4.330	65.37	3154.7	3.236	49.13
0.588	7.571	177.21	7816.2	6.180	37.87
0.600	9.278	208.74	9577.3	7.279	36.40
0.573	4.223	64.15	3071.5	3.175	49.51
0.561	8.284	164.24	8551.9	5.728	32.08
0.606	8.709	177.06	8990.3	6.175	32.89
0.574	8.539	167.29	8814.6	5.834	31.70
0.590	3.288	49.31	2391.5	2.441	49.00
0.560	9.784	171.02	10101.0	5.964	28.28
0.580	3.200	46.415	2333.7	2.297	48.00

TABLE 9

Foam Cement Flow Data

Foam Cement Quality: $0.60 < \Gamma < 0.65$

<u>Quality Fraction</u>	<u>Velocity Ft/Sec.</u>	<u>Pressure Drop ΔP psi</u>	<u>Shear Rate $(8v/D)$ Sec^{-1}</u>	<u>Shear Stress $(D\Delta P/4L)$ psf</u>	<u>Viscosity cp.</u>
0.60	3.325	61.25	2418.7	3.0318	60.03
0.60	3.337	52.26	2426.9	2.5868	51.05
0.60	3.318	49.70	2413.4	2.460	49.00
0.61	3.976	60.04	2892.1	2.972	49.50
0.62	8.091	171.91	8352.1	5.995	34.38
0.65	9.014	206.43	9304.6	7.199	37.06
0.65	9.139	186.64	9434.1	6.509	33.04
0.61	9.454	201.42	9759.4	7.025	34.47
0.61	8.101	147.74	8363.3	5.1522	29.50
0.62	8.227	157.17	8492.5	5.4813	30.91
0.63	8.566	196.46	8843.2	6.851	37.11
0.63	7.322	164.29	7558.4	5.729	36.30
0.65	7.599	177.06	7844.7	6.175	37.70
0.62	7.081	177.11	7309.6	6.176	40.47
0.61	3.434	52.85	2495.7	2.616	50.20
0.62	3.490	55.11	2539.6	2.728	51.44
0.61	3.386	52.60	2462.7	2.603	50.60
0.62	3.481	54.32	2532.2	2.688	50.86
0.63	3.516	57.71	2557.1	2.856	53.50

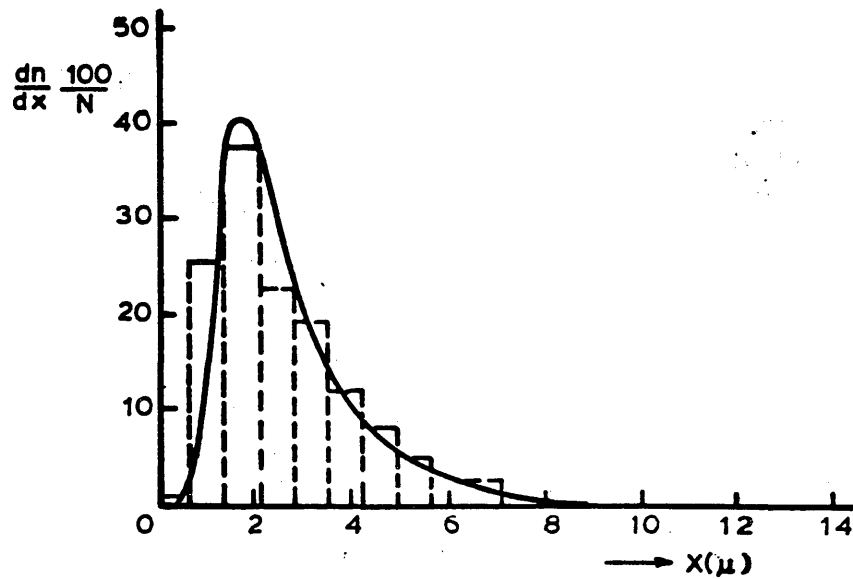


Fig. 1. Continuous Distribution Curve ($a=8.7\mu$ and $X=19\mu$), after Becher (1957)

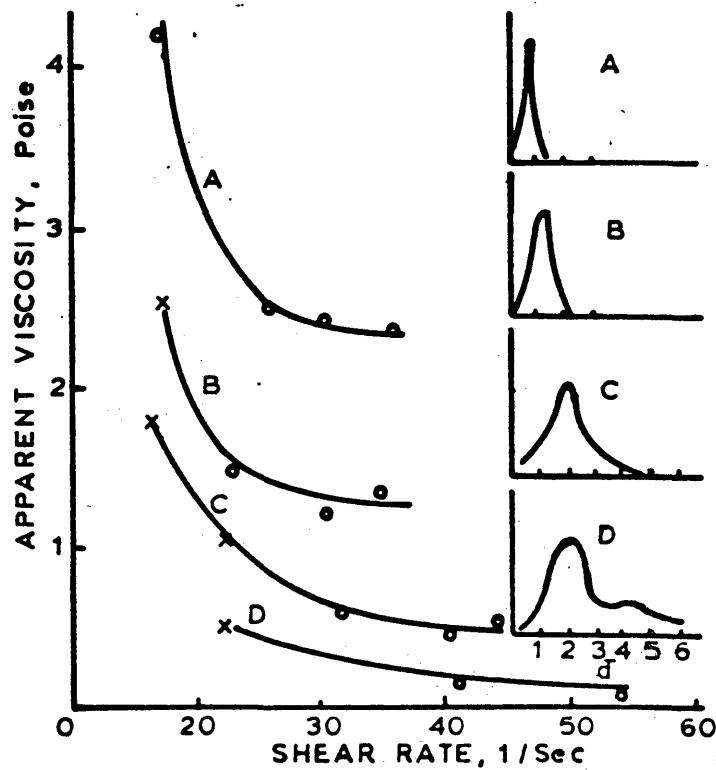


Fig. 2. Apparent Viscosity at Different Rate of Shear of Emulsions Whose Size Distribution Curves are Shown as Insets, after Richardson (1953).

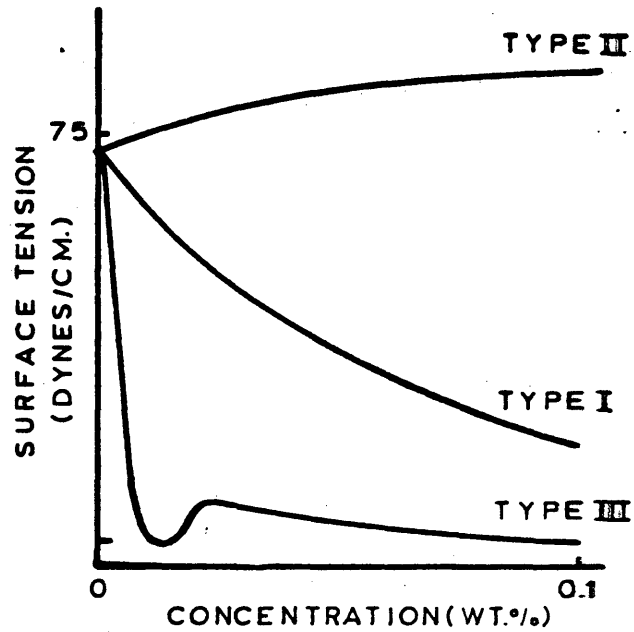


Fig. 3. Schematic representation of the principal types of surface tension concentration curves, after McBain, Ford, and Wilson (1937).

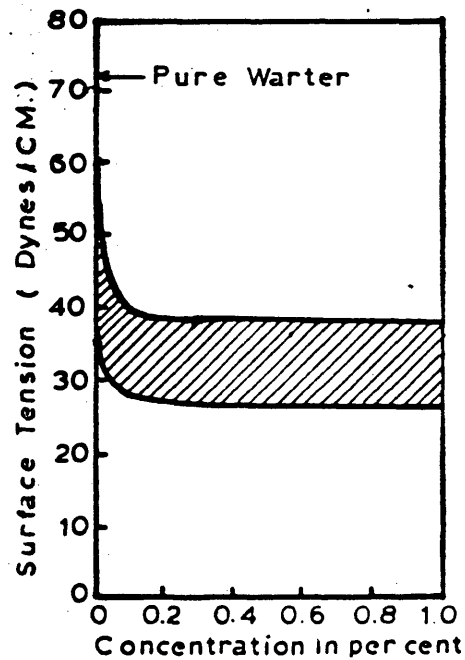


Fig. 4. The range of surface tensions found in solutions of most surface-active compounds, after Fischer (1946).

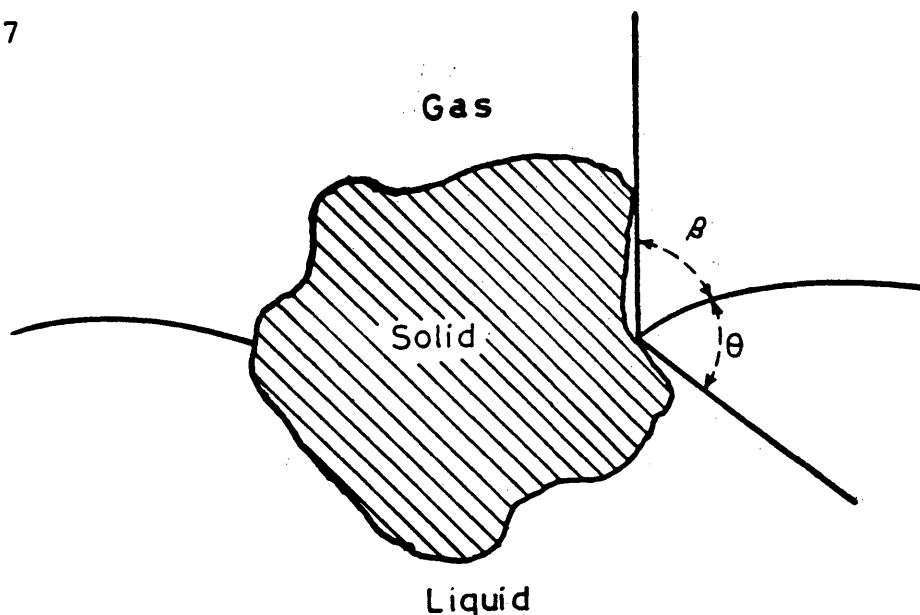


Fig. 5. Solid particles suspended in gas-liquid boundary by surface tension. β is the angle formed by the vertical with liquid surface at a point of the 3-phase line, and θ is the contact angle at this point, after Bikerman (1973).

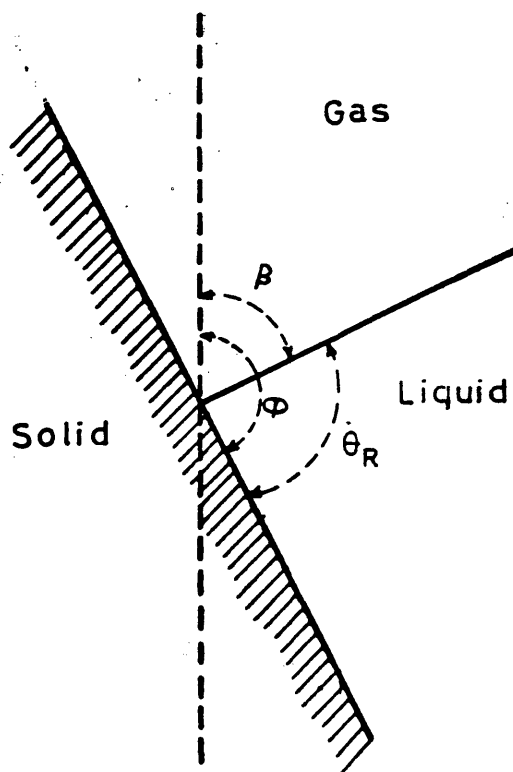


Fig. 6. Relation between the three angles β (between the vertical and the liquid surface), ψ (between the vertical and the solid profile), and θ_R (the receding contact angle), after Bikerman (1973).

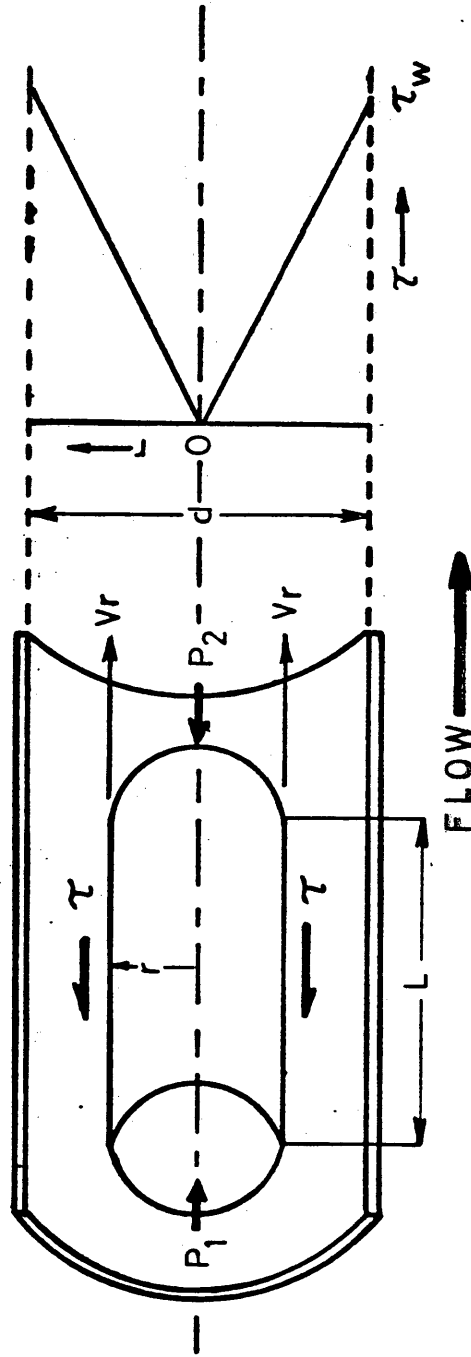


FIG: 7. Rabinowitsch Flow Model

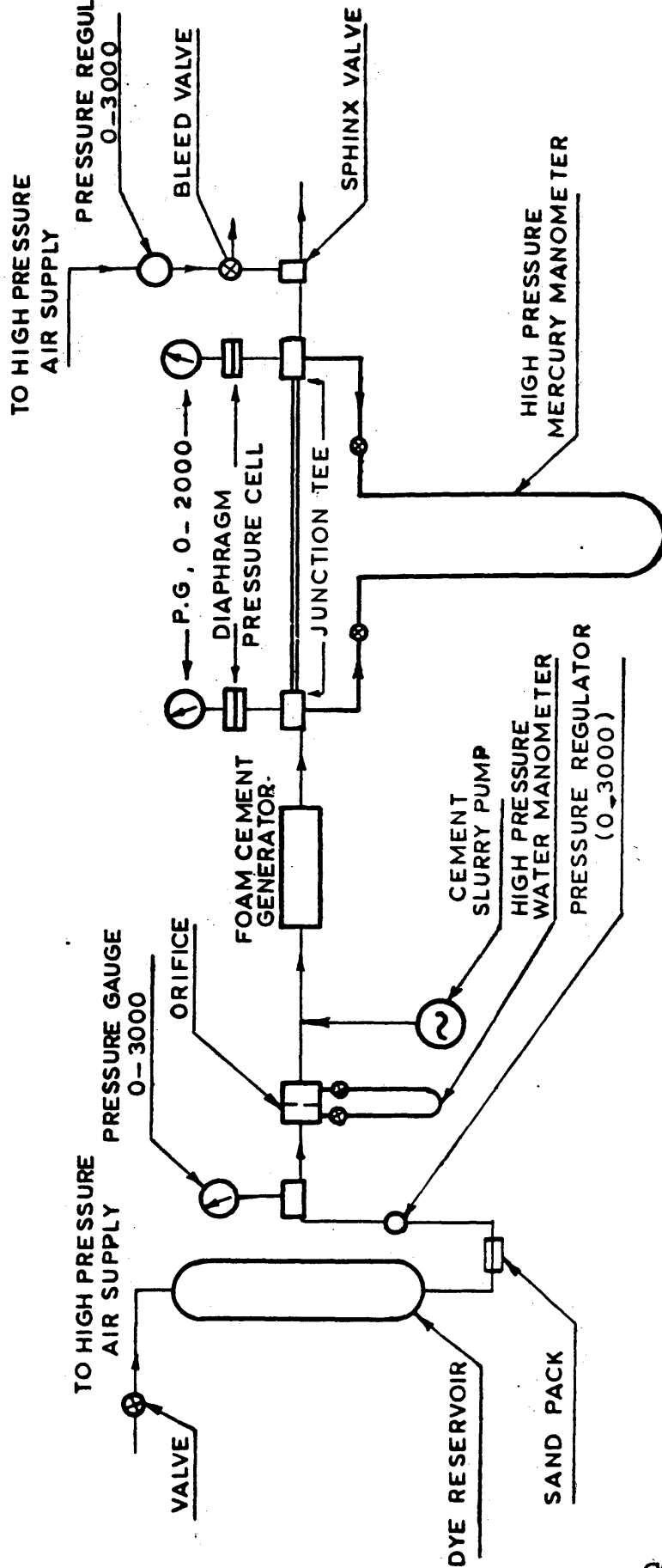


FIG : 8. HIGH PRESSURE TEMPERATURE VISCOMETER

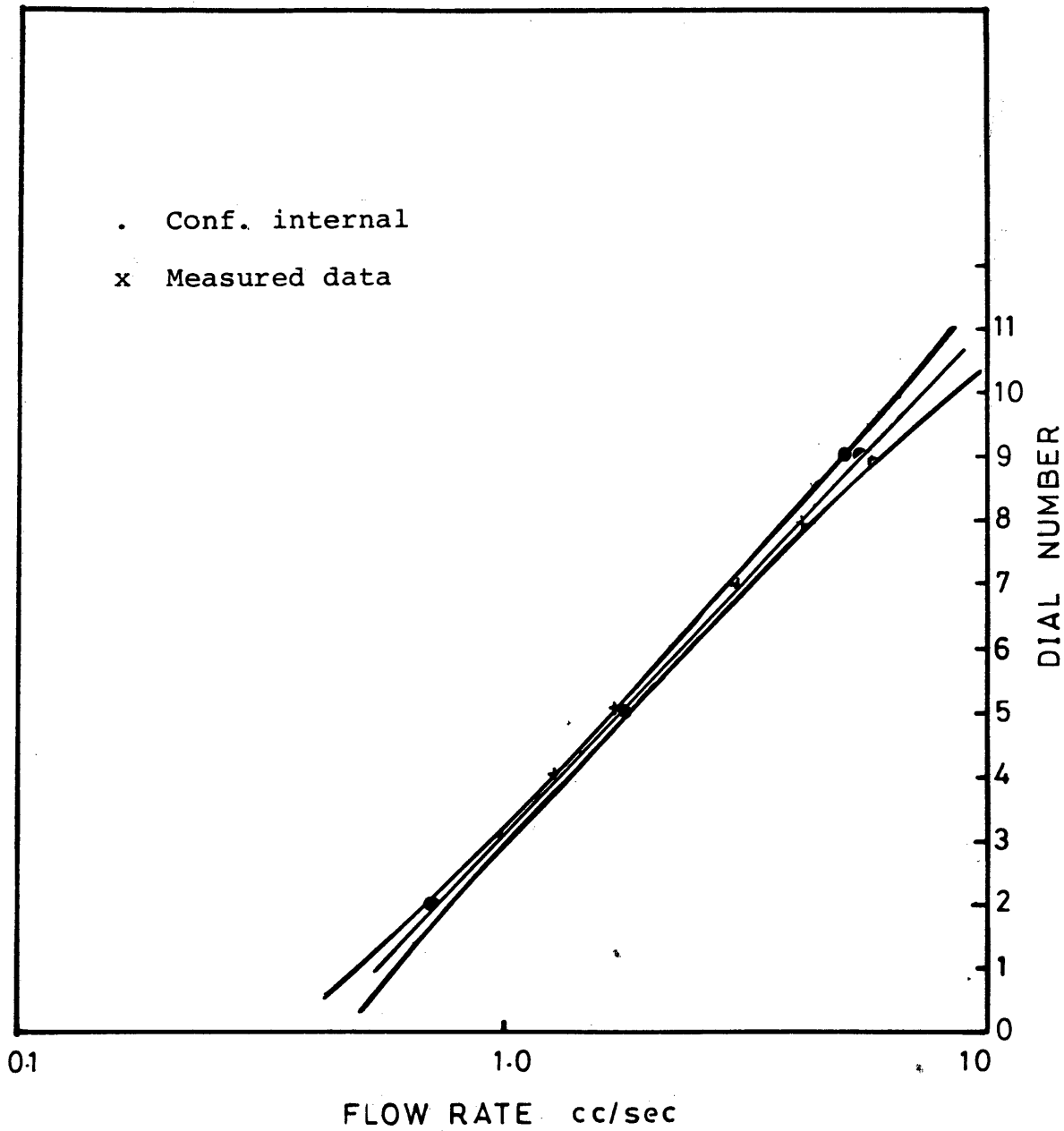


FIG. 9. Plot of pump flow rate versus dial number with upper and lower 95 percent confidence limit.

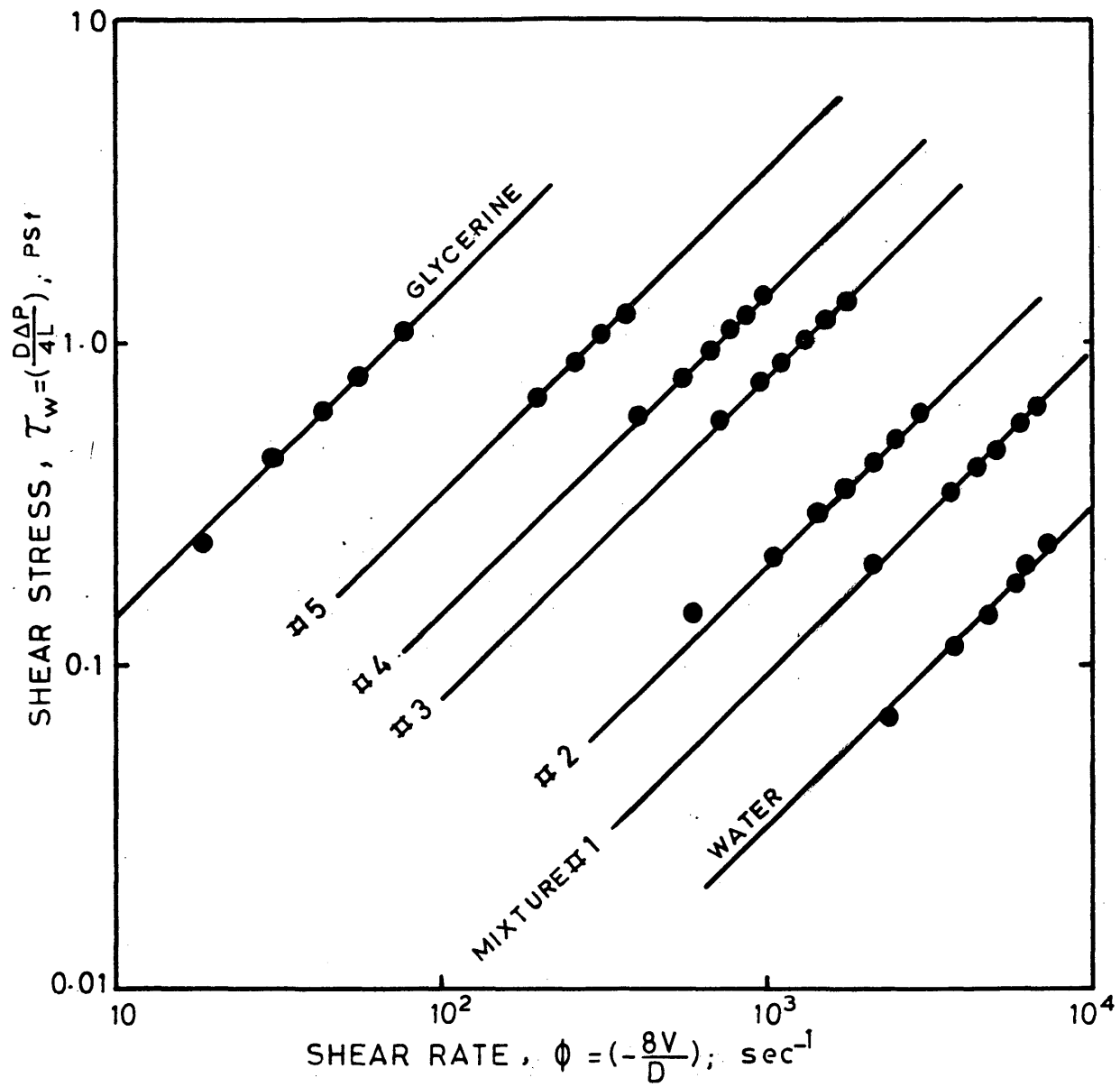


FIG. 10: CALIBRATION OF TUBES

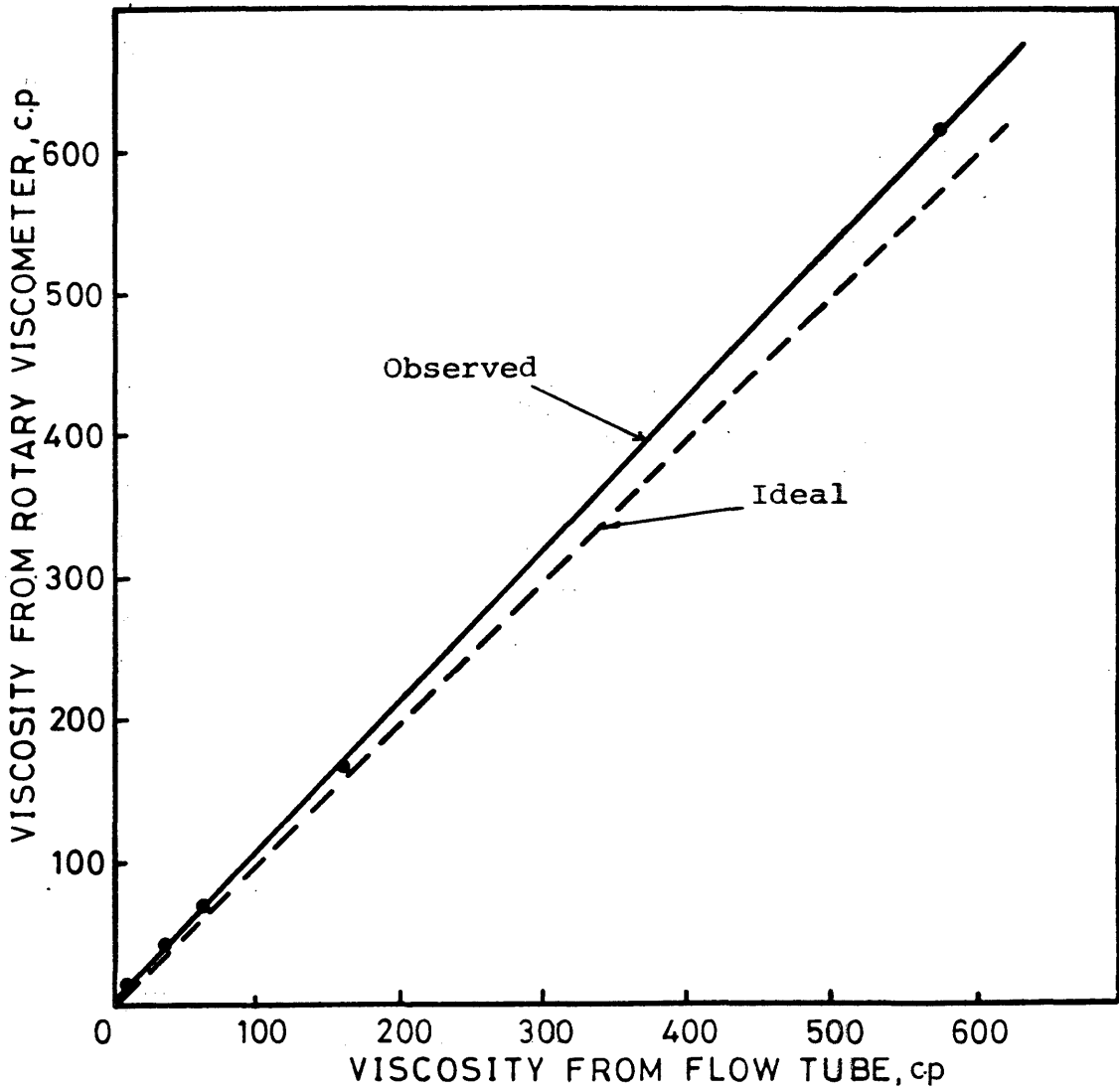


FIG: 11. VISCOSITY CALIBRATION CURVE

T-1887

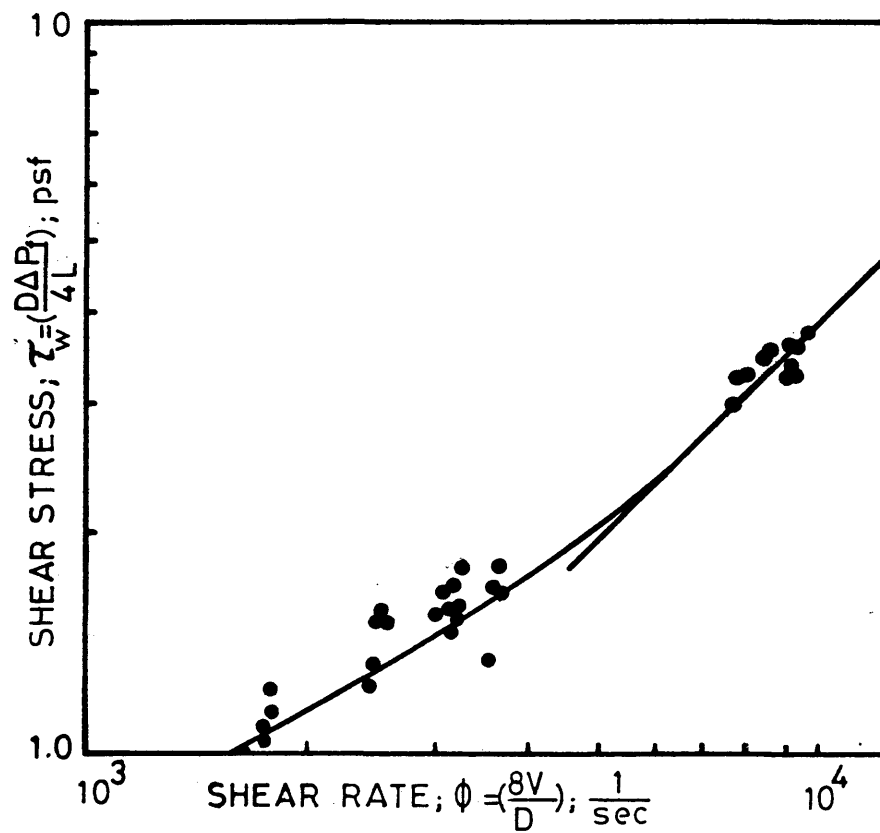


FIG:12. FOAM CEMENT RHEOLOGY DIAGRAM
($30 < \Gamma < 40$)

T-1887

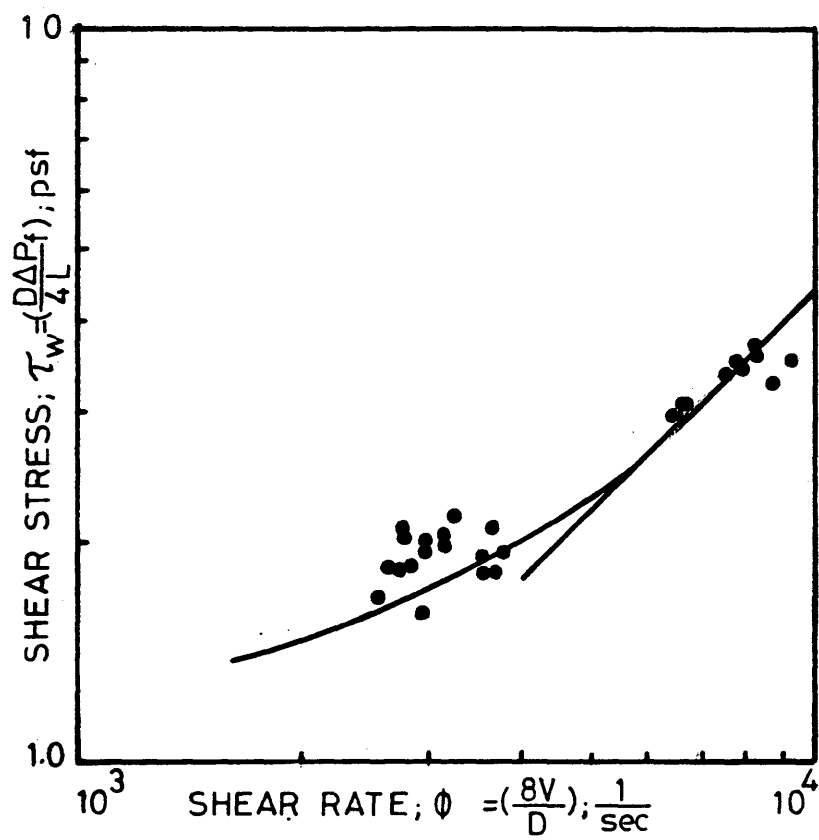


FIG:13. FOAM CEMENT RHEOLOGY DIAGRAM

$$40 < \Gamma < 45$$

T-1887

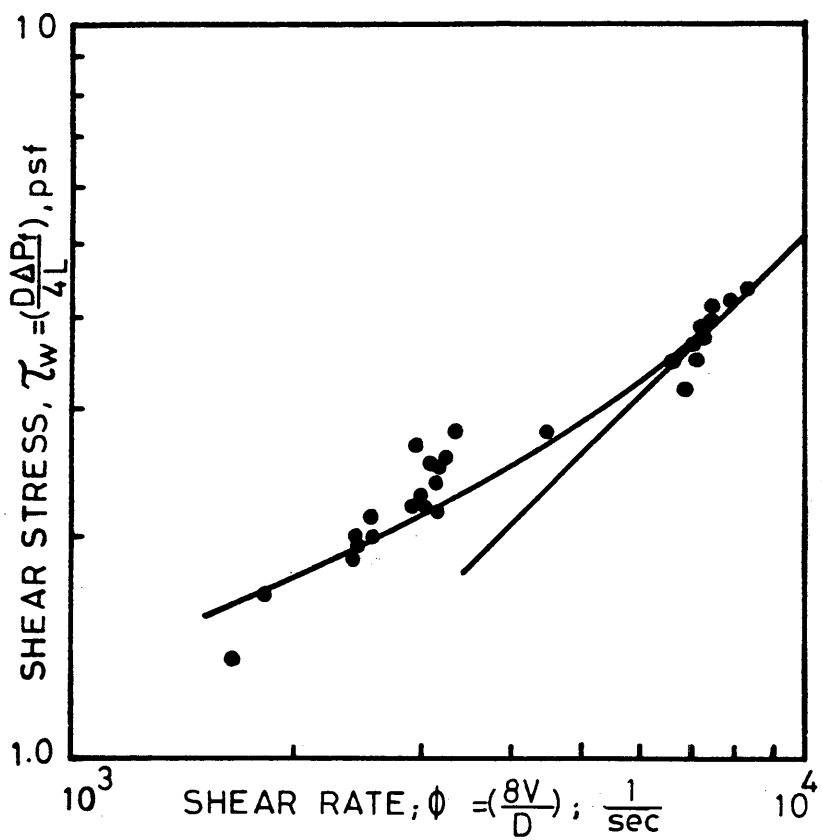


FIG:14. FOAM CEMENT RHEOLOGY DIAGRAM

 $(45 < \Gamma < 50)$

T-1887

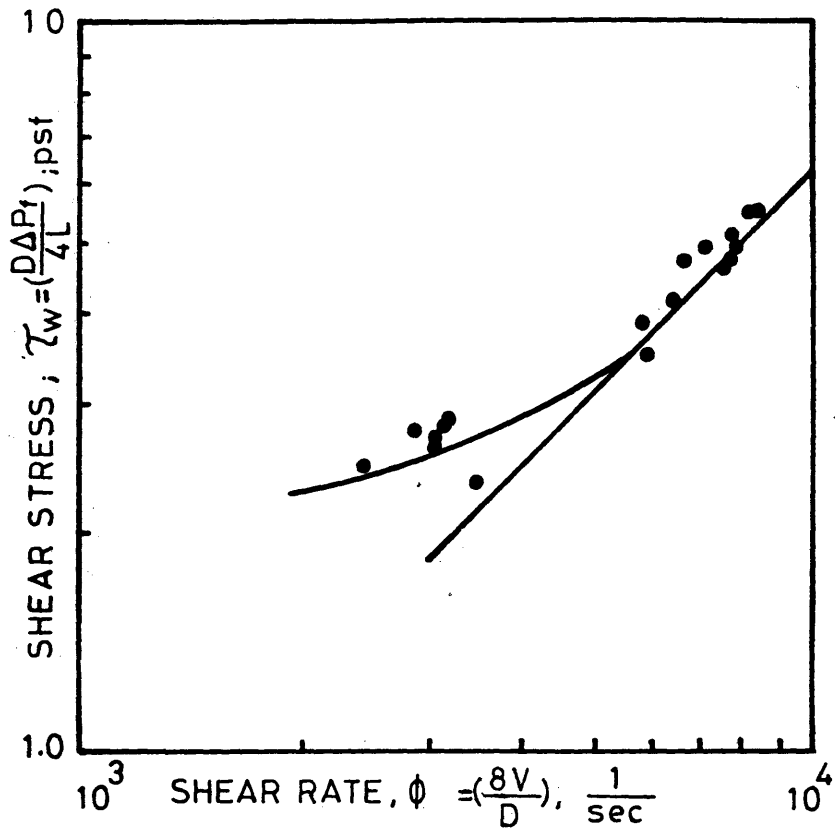


FIG: 15.FOAM CEMENT RHEOLOGY DIAGRAM
($50 < \Gamma < 55$)

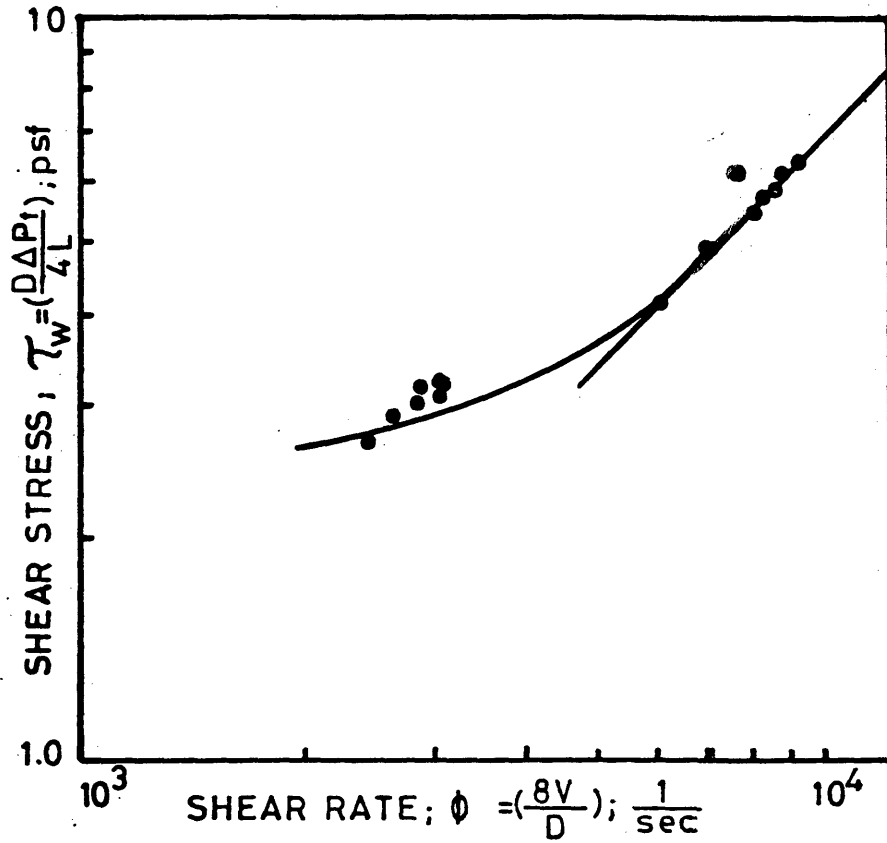


FIG: 16. FOAM CEMENT RHEOLOGY DIAGRAM

(55 Γ 60)

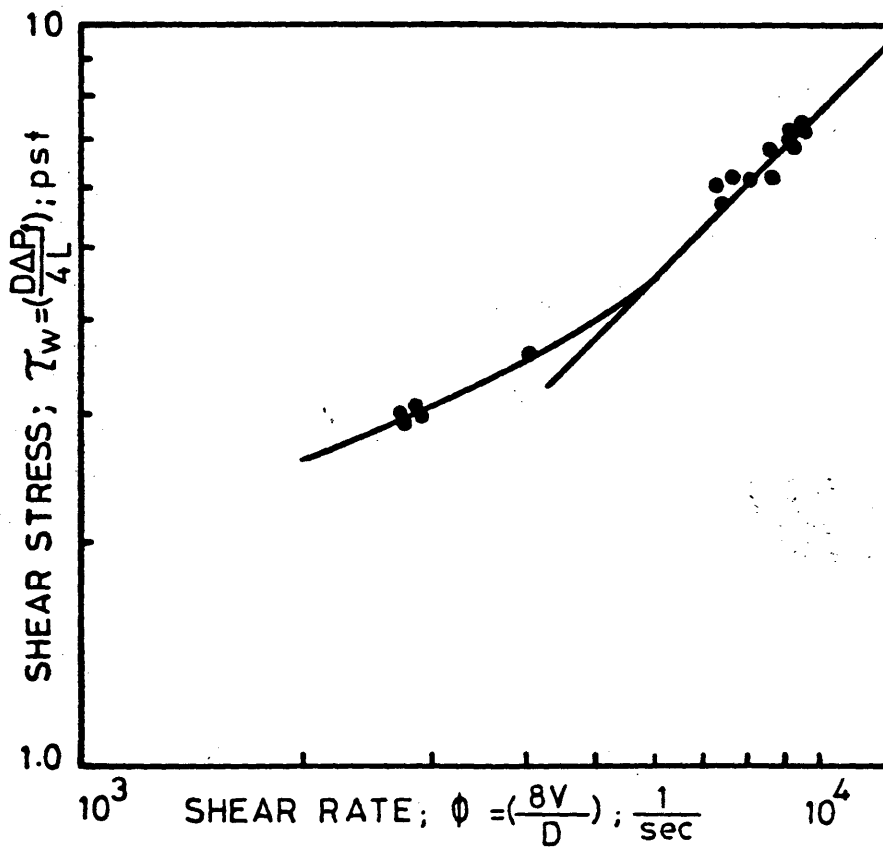


FIG:17. FOAM CEMENT RHEOLOGY DIAGRAM

(60 < Γ < 65)

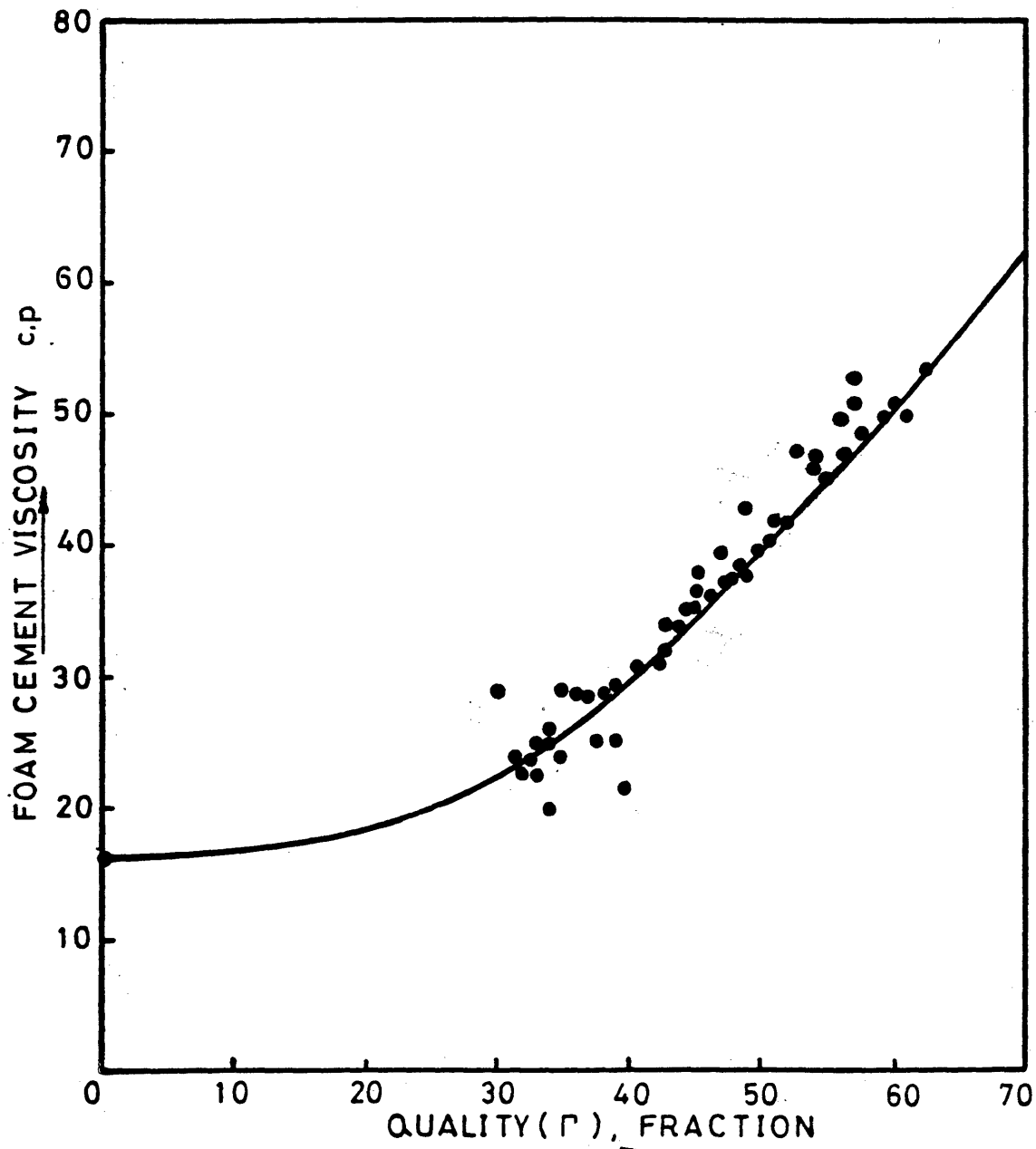


FIG:18. FOAM CEMENT VISCOSITY
(TUBE I.D. _ 0.132)

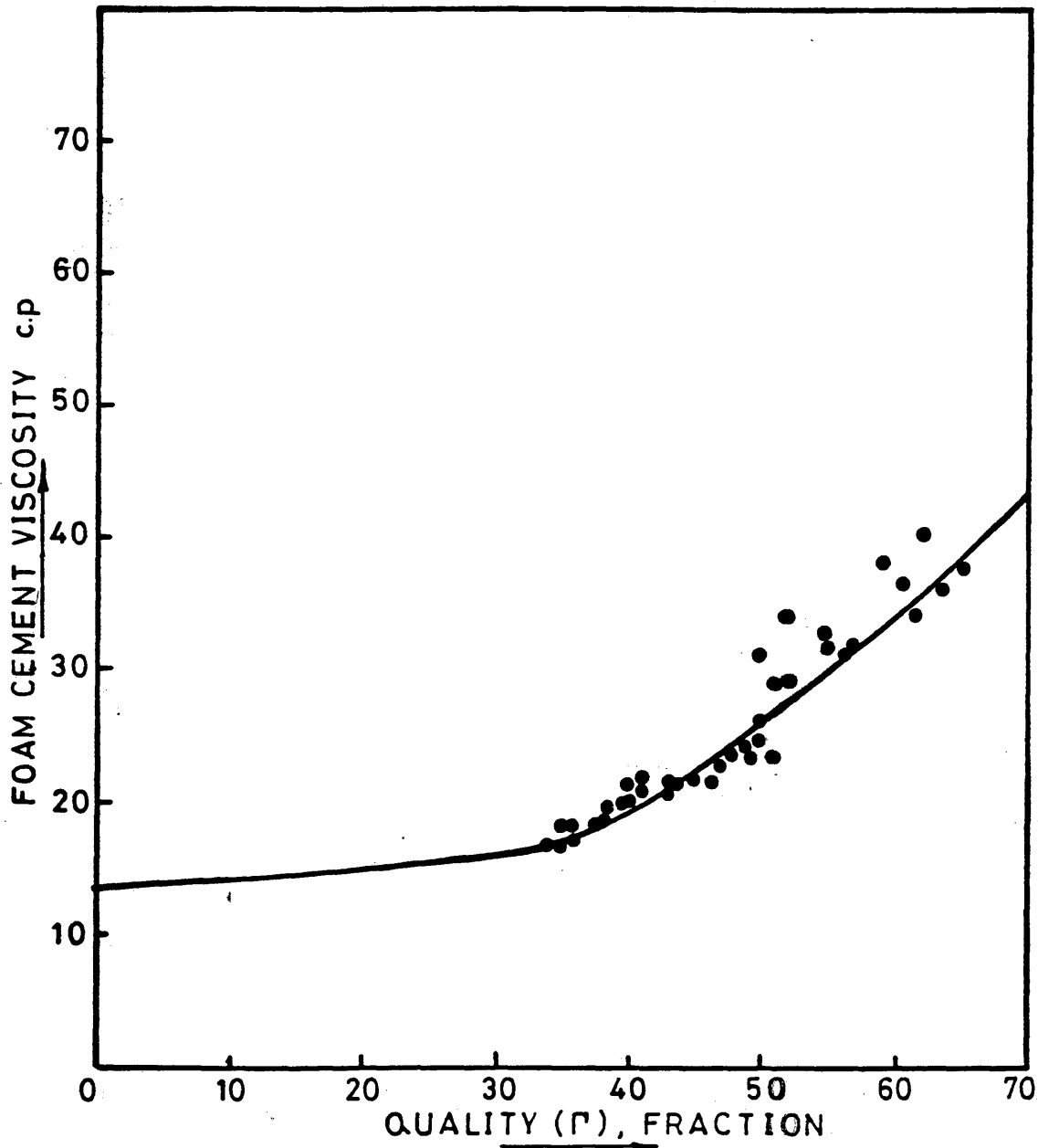


FIG :19. FOAM CEMENT VISCOSITY
(TUBE I.D. - 0.093)

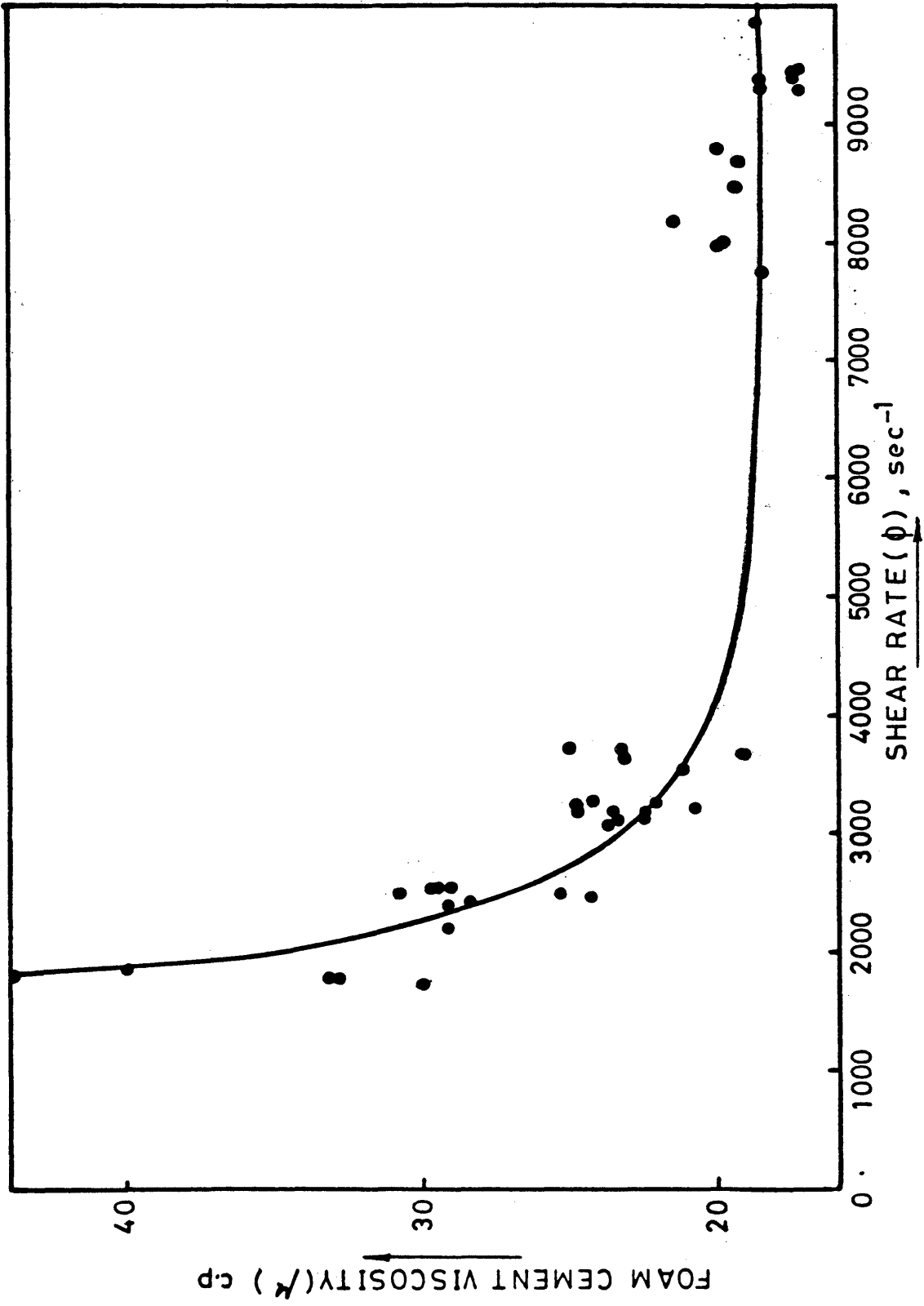


FIG: 20. FOAM CEMENT VISCOSITY
(0.30 < Γ < 0.40)

5

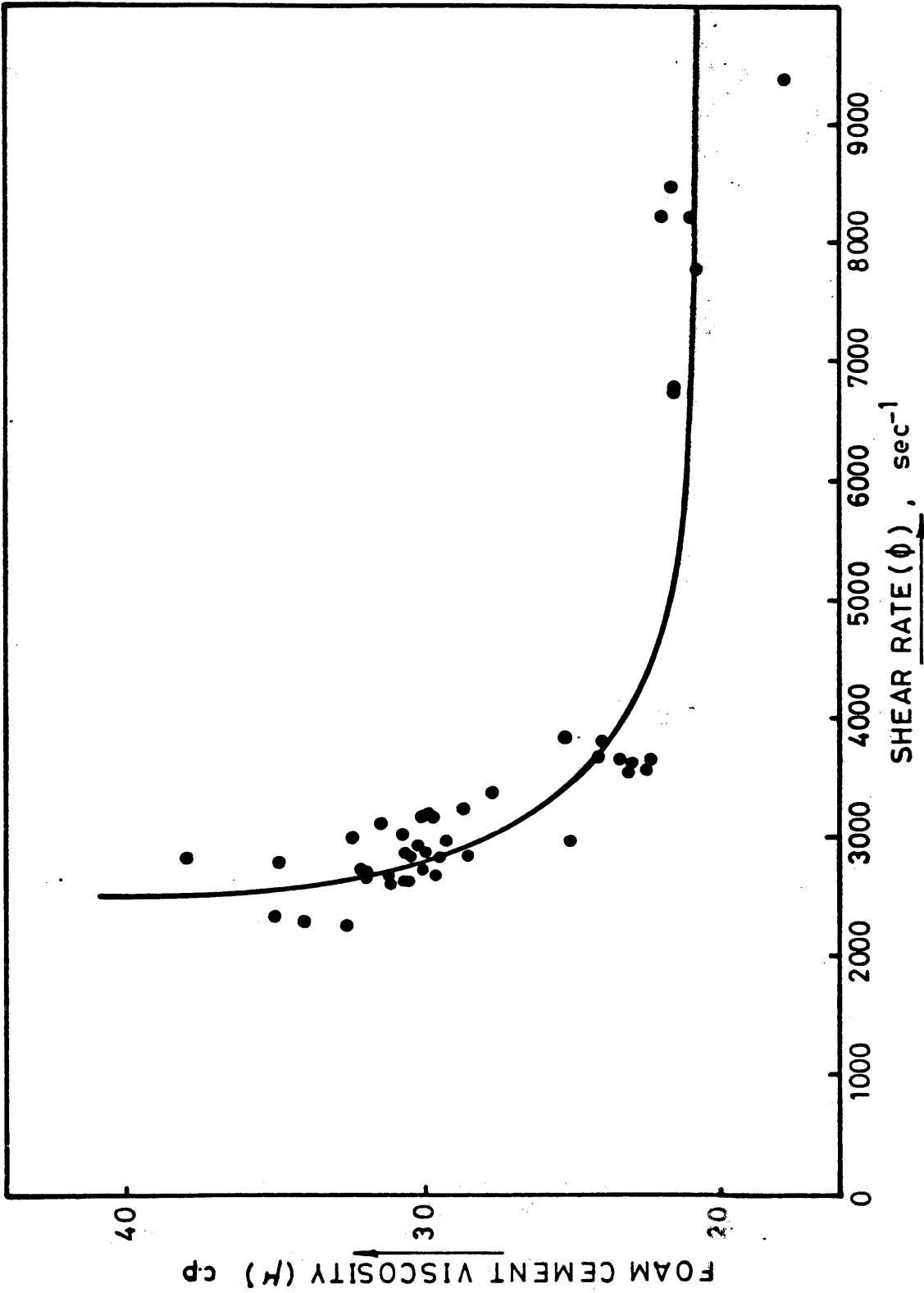


FIG:21. FOAM CEMENT VISCOSITY; ($0.40 < \Gamma < 0.45$)

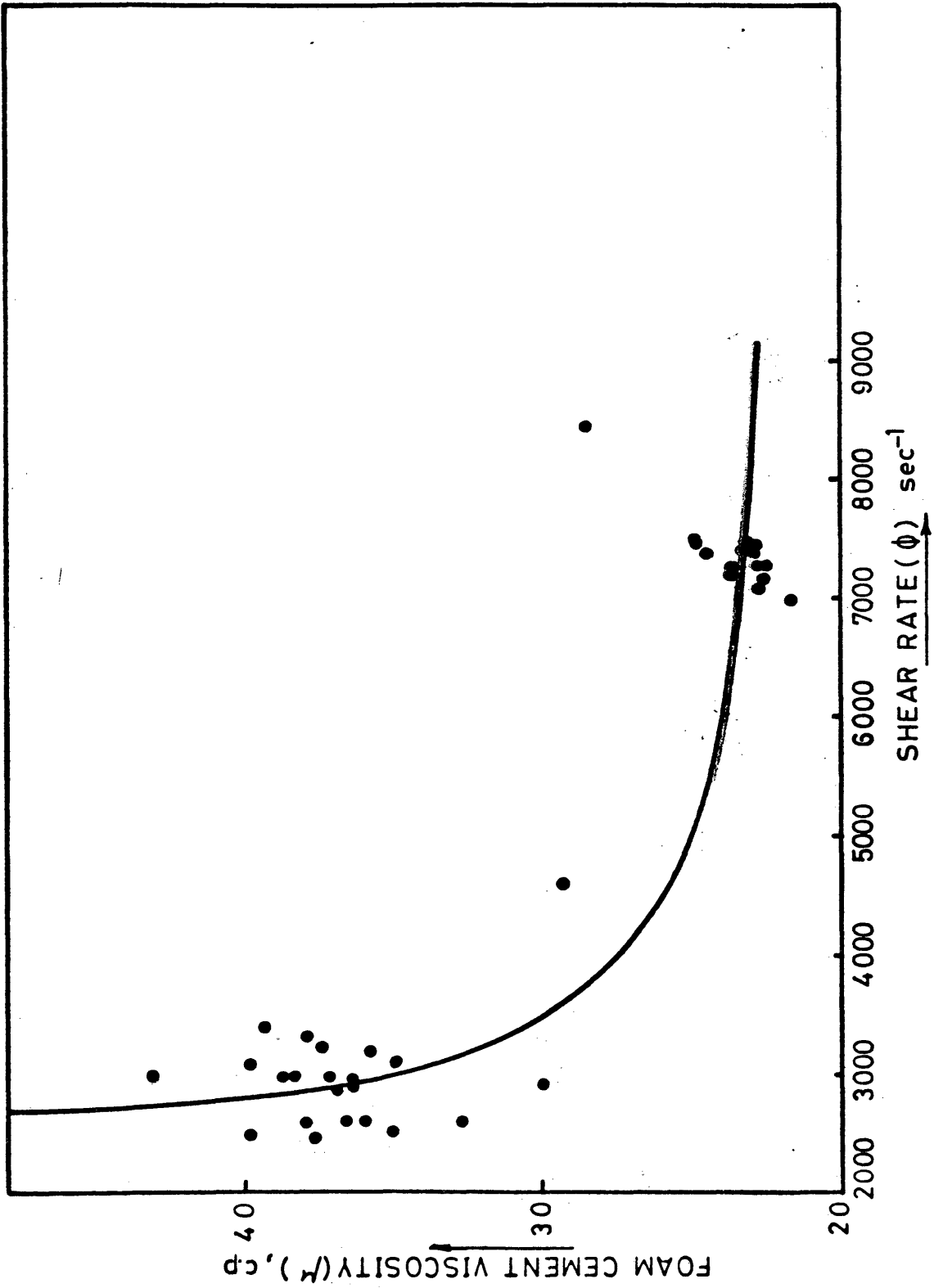


FIG: 22. FOAM CEMENT VISCOSITY , ($0.45 < \Gamma < 0.50$)

ARTHUR LAKES LIBRARY
COLORADO SCHOOL of MINES
GOLDEN, COLORADO 80401

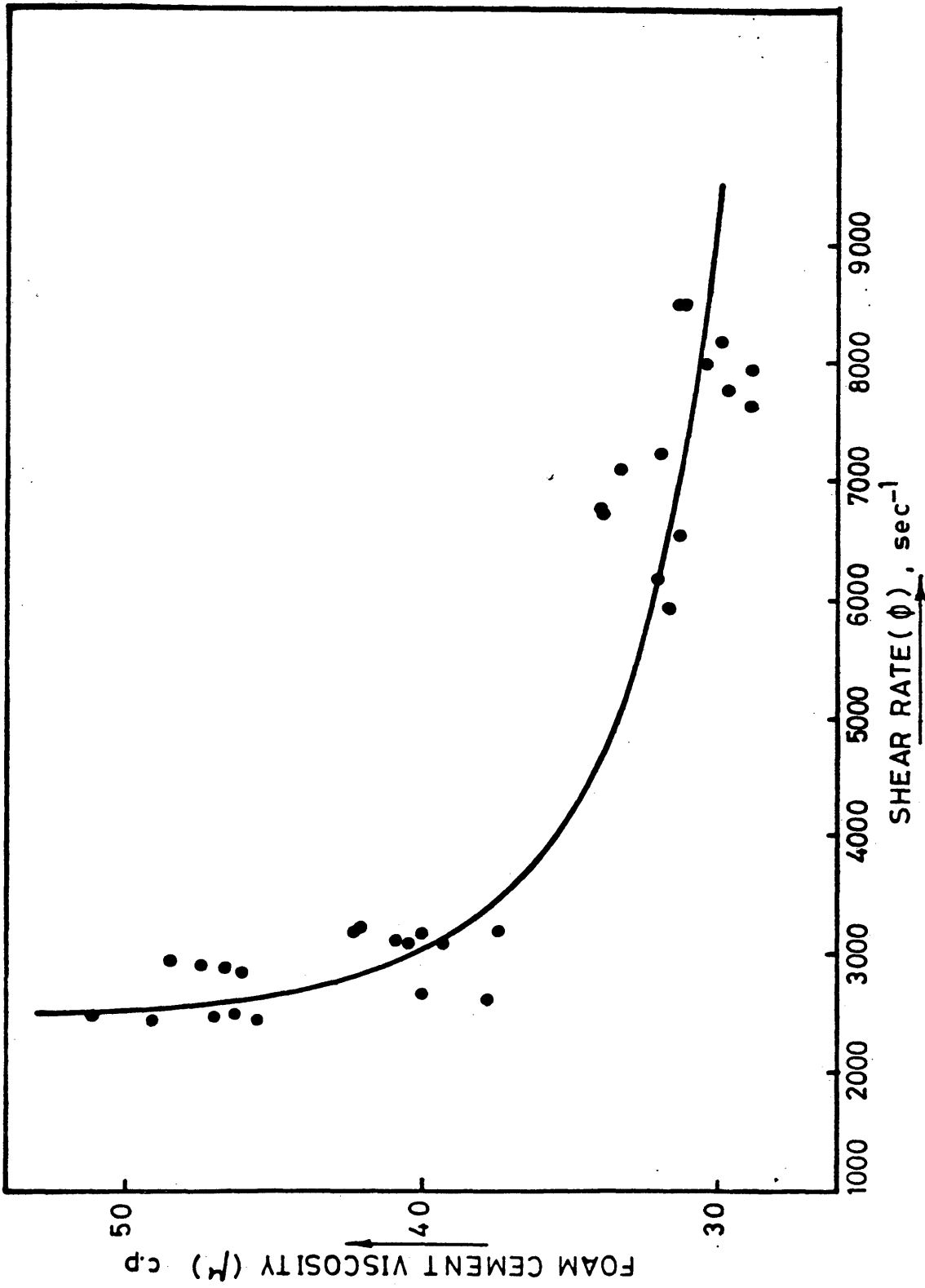


FIG: 23. FOAM CEMENT VISCOSITY, (0.50 Γ <math>< 0.55 </math>)

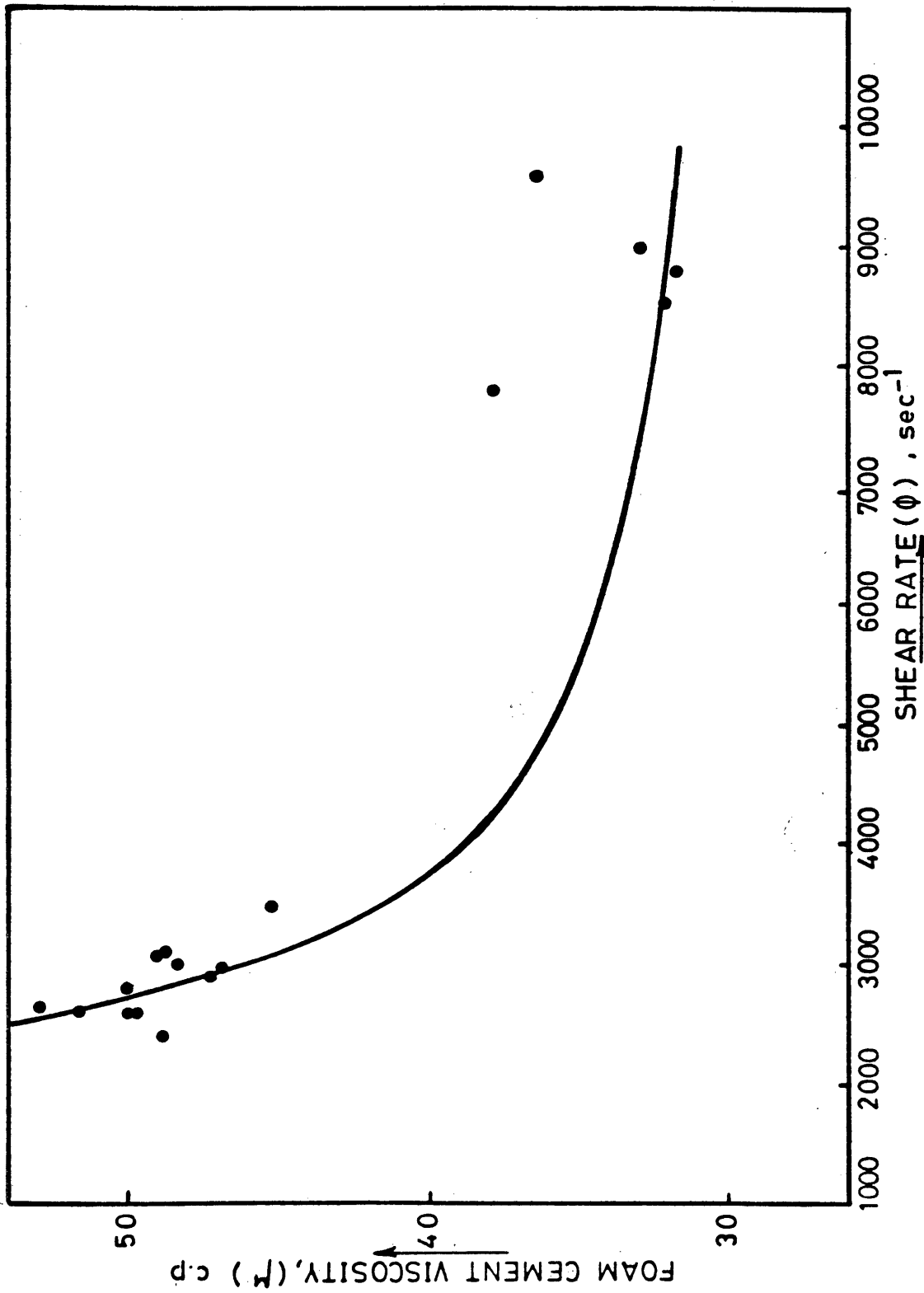


FIG: 24. FOAM CEMENT VISCOSITY, (0.55 Γ <math>< 0.60</math>)

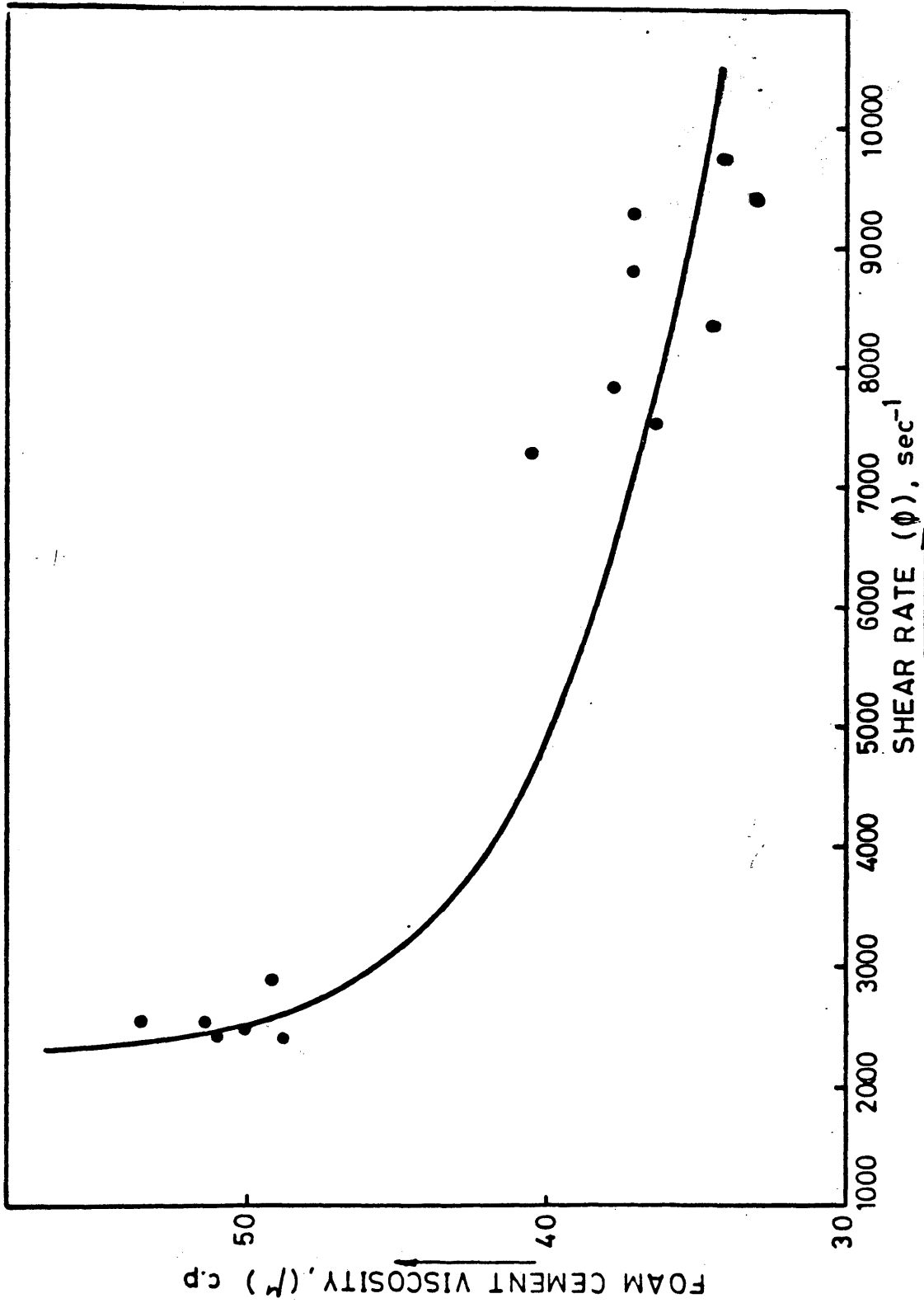


FIG: 25. FOAM CEMENT VISCOSITY, (0.60 Γ <math>< 0.65</math>)

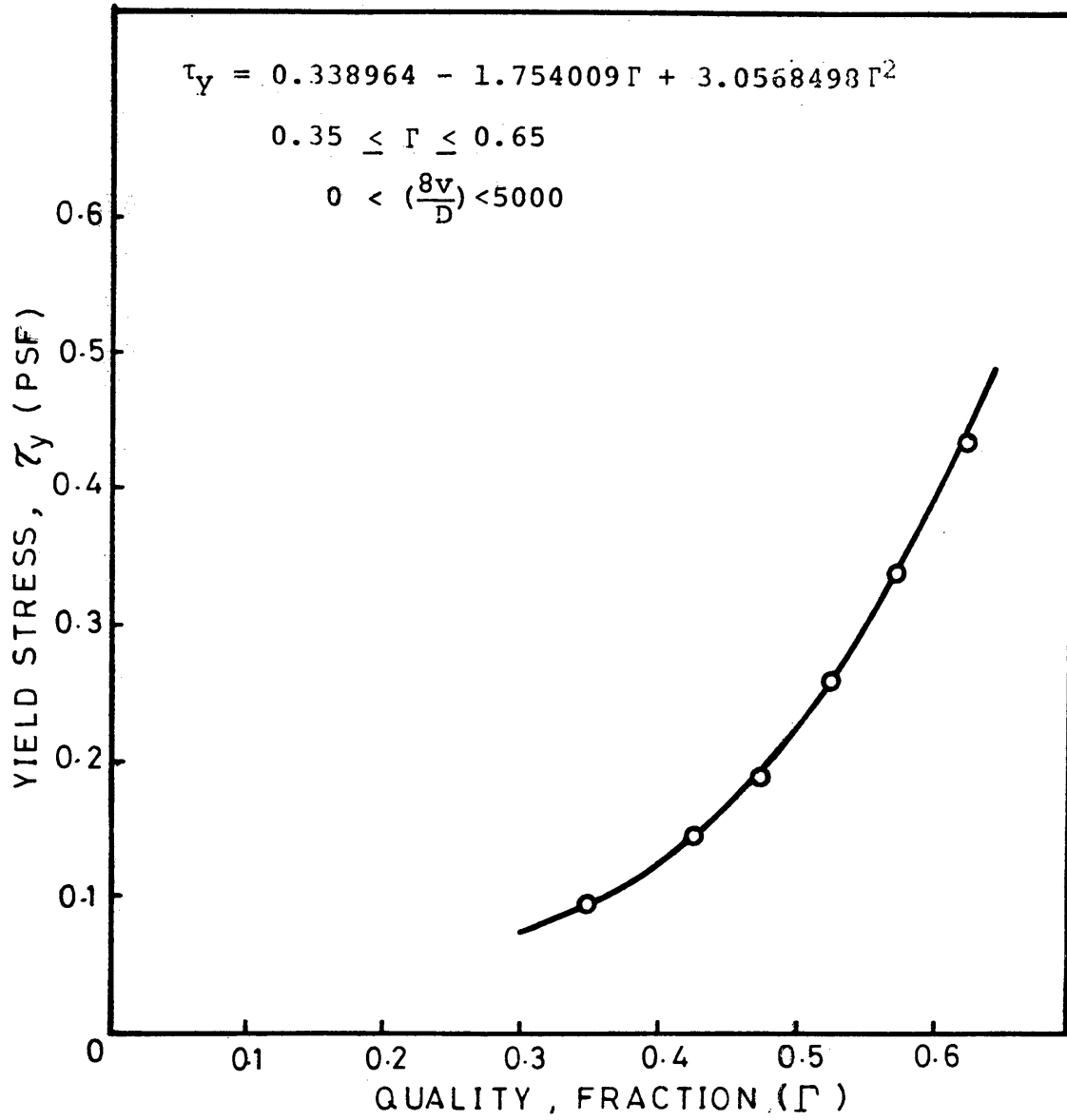


FIG. 26. YIELD STRESS OF FOAM CEMENT

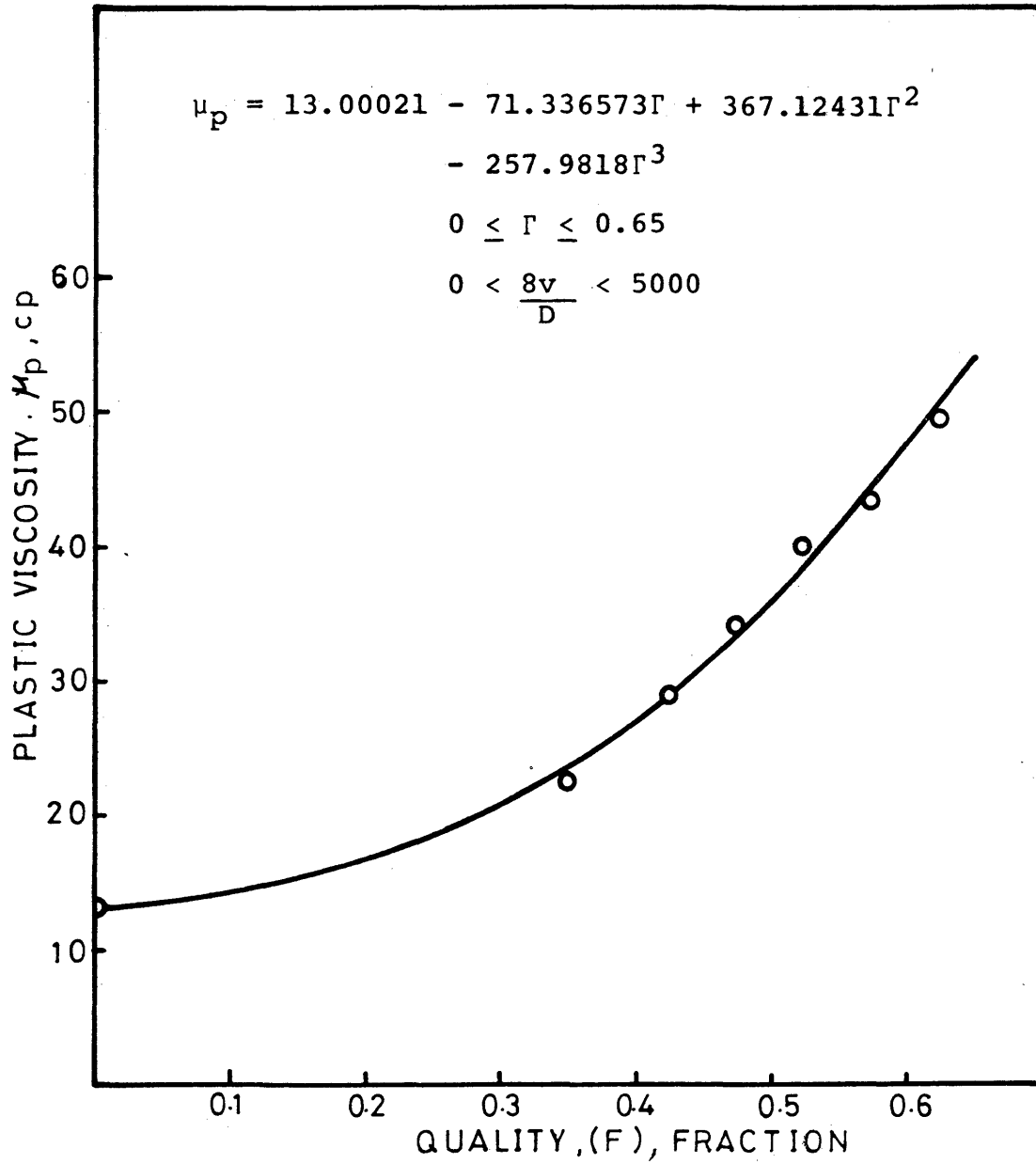


FIG. 27. PLASTIC VISCOSITY OF FOAM CEMENT

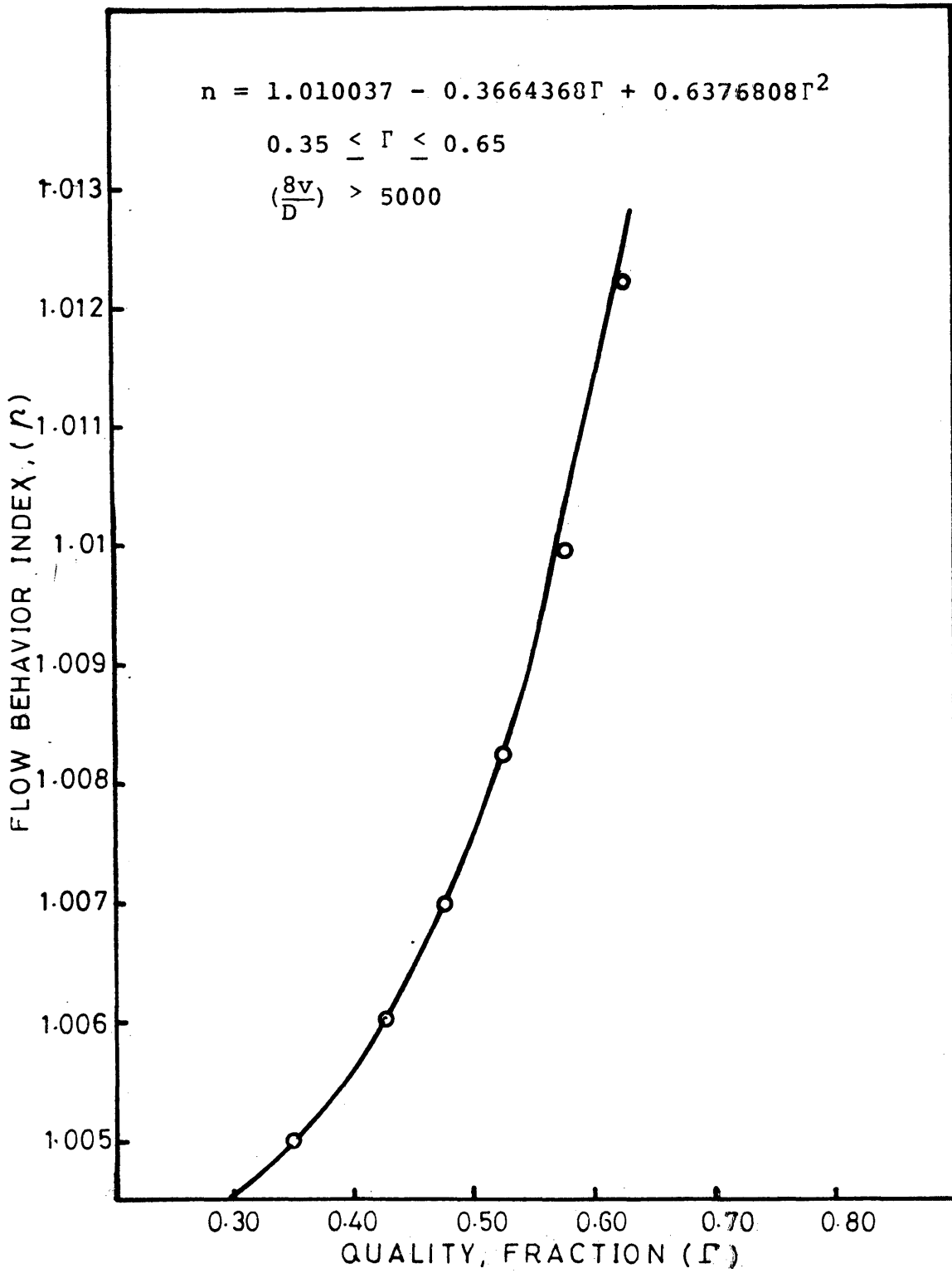


FIG: 28. FLOW BEHAVIOR INDEX OF FOAM CEMENT

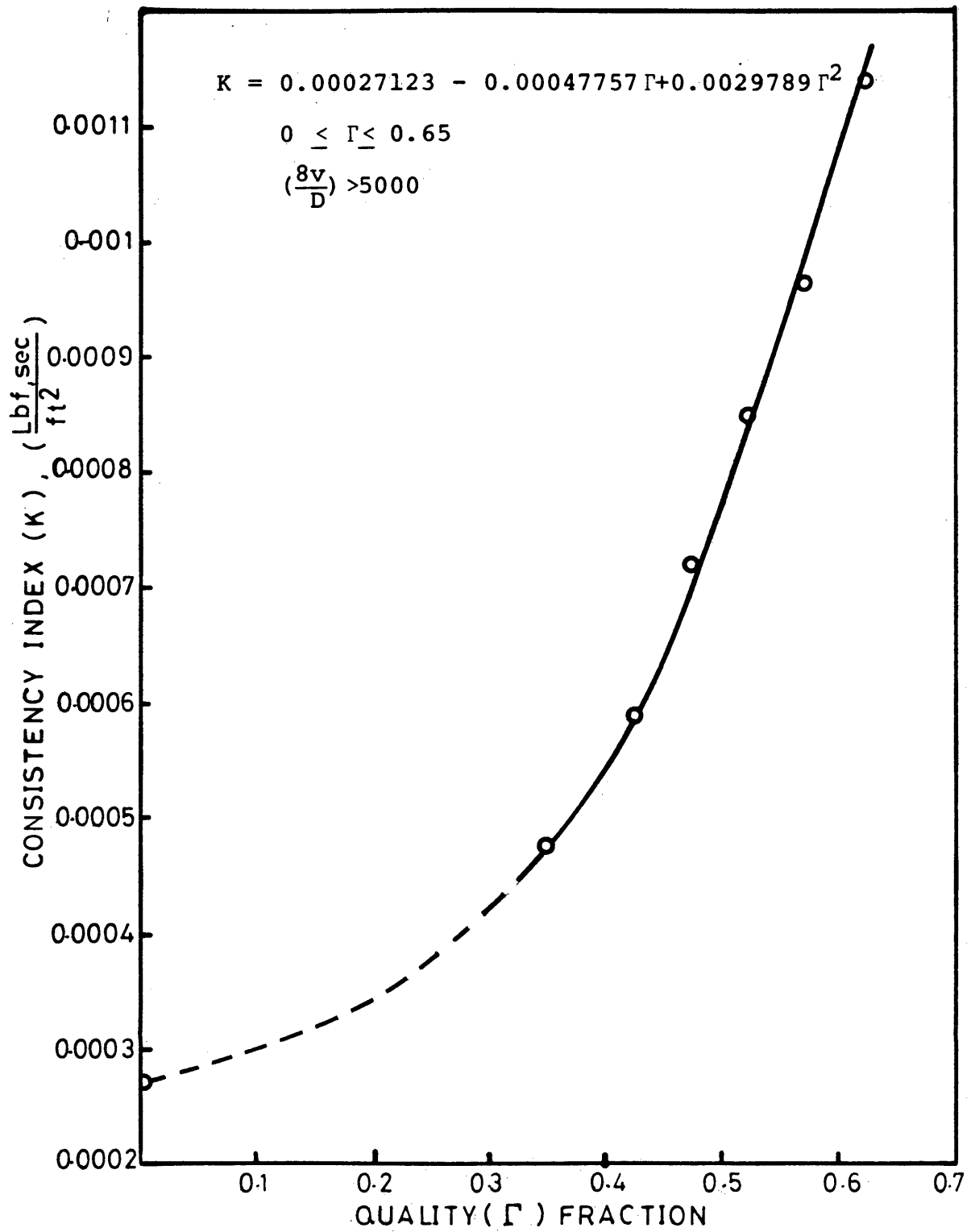


FIG. 29. CONSISTENCY INDEX OF FOAM CEMENT

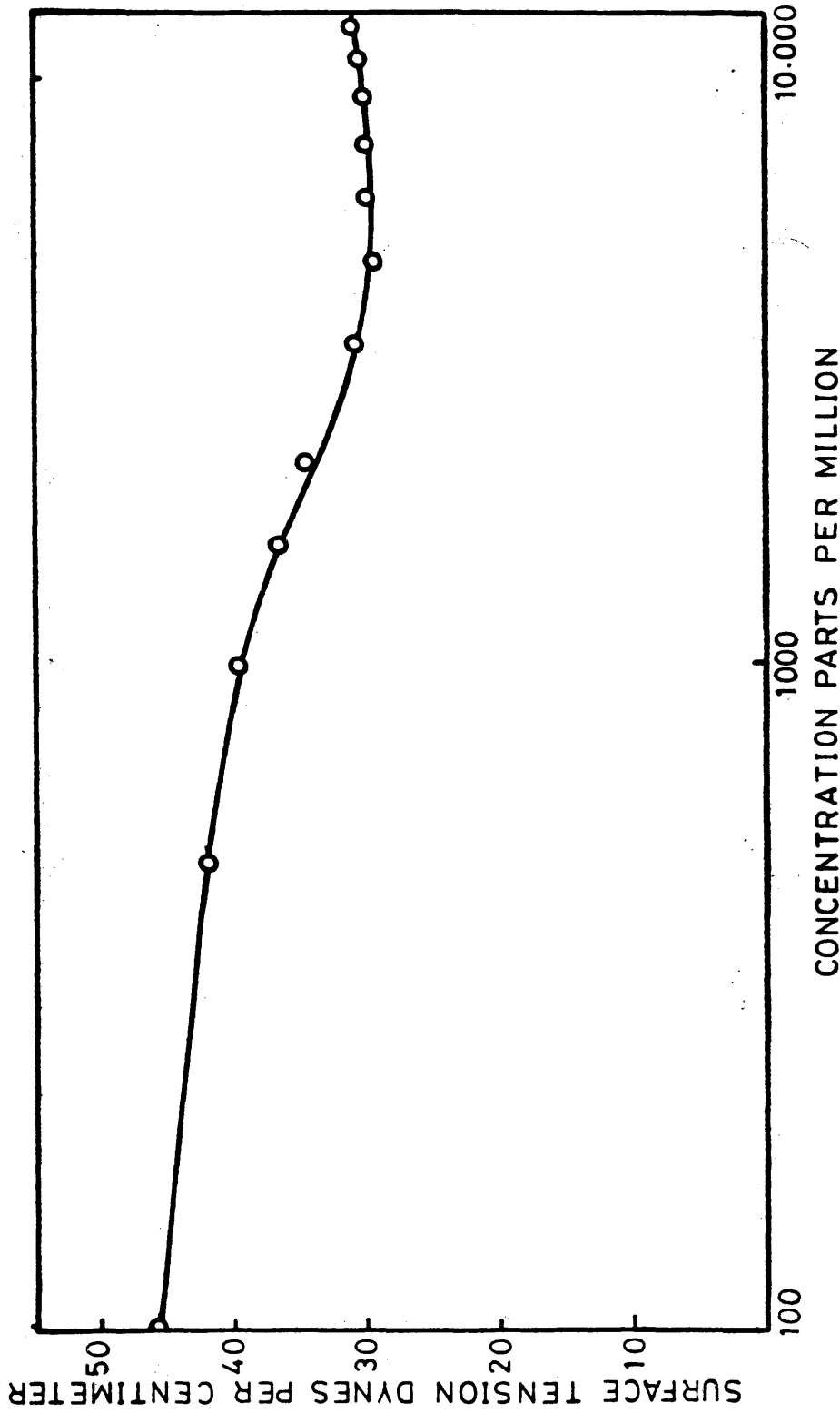


FIG. 30. SURFACE TENSION OF HOWCO AND TAP WATER

ARTHUR LAKES LIBRARY
COLORADO SCHOOL OF MINES
GOLDEN, COLORADO 80401